Theoretical Analysis of Nitroxide-Mediated Copolymerization of Styrene and α-Methyl-Styrene under Different Operating Policies and Reactor Designs

Cecilia Fortunatti,* Claudia Sarmoria, Adriana Brandolin, Mariano Asteasuain

The polymerization that IUPAC terms reversible-deactivation radical polymerization is a controlled radical polymerization technique (CRP) that allows producing polymers with tailored properties without the stringent conditions typical in ionic polymerization. A theoretical analysis is presented of the influence of operating and design conditions on the product properties for the nitroxide-mediated copolymerization (NMP) of styrene and α-methyl styrene. Several reactor configurations are analyzed, with different feeding policies and temperature profiles. To this end a mathematical model is developed to predict copolymer average properties and the complete bivariate MWD. The results help establishing design parameters and optimal operating policies to obtain desired copolymer microstructures.

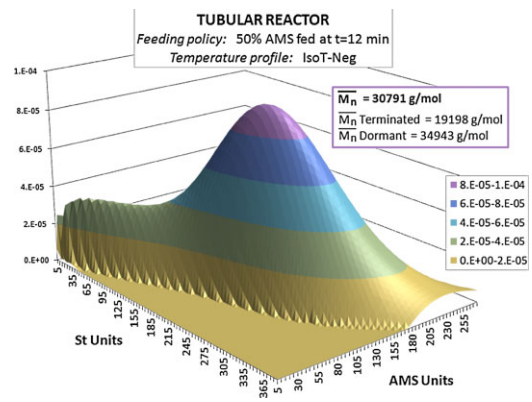

1. Introduction

Since their discovery in the early 1990s, controlled radical polymerization (CRP) techniques have attracted great interest in scientific and industrial practitioners because they combine advantages of both ionic and radical polymerizations. Their use has the potential of allowing production of unique materials in a relatively simple way at industrial scales, since the reaction set-up is straightforward and the conditions are mild, while affording a level of control unprecedented in radical polymerizations.

In CRP, the contribution of termination reactions is minimized and the apparently simultaneous growth of all chains can be achieved thanks to a fast initiation and the subsequent establishment of a dynamic equilibrium between propagating radicals and various dormant species. Consequently, most polymer chains are initiated in a relatively short period of time and then grow slowly. The interactions between growing radicals are limited through the action of an agent that can deactivate them reversibly, while the total effect of termination is reduced through the low concentration of active chains. Hence, individual chains may take hours to grow.[1,2]

C. Fortunatti, Prof. C. Sarmoria, Prof. A. Brandolin, Prof. M. Asteasuain
Planta Piloto de Ingeniería Química (PLAPIQUI), UNS-CONICET, Camino La Carrindanga km 7, 8000 Bahía Blanca, Argentina
E-mail: cfortunatti@plapiqui.edu.ar

Copolymerization by means of CRP techniques, or controlled radical copolymerization (CRcoP), is of particular importance since, unlike ionic polymerization, several comonomer pairs react by this mechanism. Besides, a large number of polymer products can be designed by changing the comonomers and their relative amounts in the final copolymer. CRcoP allows obtaining not only block, graft, gradient, and statistical copolymers but also complex architectures such as star and comb polymers. Statistical copolymers have special characteristics due to the distinctive kinetic features of CRcoP. In the reacting medium comonomers are consumed at different rates according to their reactivity ratios. Therefore, when chains are generated at different times (as in conventional radical copolymerization) the composition drifts with conversion, leading to composition differences among polymer chains generated at different times. By contrast, the gradual growth characteristic of CRcoP yields copolymer products with a gradient composition distribution along chain backbones, but individual chains all have identical composition profiles (spontaneous gradient copolymer).[2,3]

It is known that the average molecular weights and the molecular weight distribution (MWD) are key properties that determine final properties of the copolymer. In addition, global and instantaneous compositions, as well as sequence length and distribution, have significant effects on the macroscopic properties of copolymers.[3,4] A model able to predict those quantities would be very useful in the design of tailor made materials.

1.1. Nitroxide-Mediated Polymerization

The three principal CRP techniques are atom transfer radical polymerization (ATRP), nitroxide-mediated polymerization (NMP), and reversible addition-fragmentation chain transfer (RAFT). NMP is one of the most studied CRP mechanisms and is based on the persistent radical effect (PRE). This effect allows the reaction to self-regulate. The essential mechanism is that the propagating radicals are rapidly trapped in a reversible deactivation process by the nitroxide (the persistent radical), forming a dormant species (alkoxyamine) that only when activated can either propagate or terminate. The reaction is strongly shifted toward the dormant species. As a result most of the polymer chains in the reaction medium will be either inactive or terminated, while the concentration of active radical chains able to propagate or terminate will be several orders of magnitude smaller. As rule of thumb, it can be said that as the proportion of dormant chains increases, the control over the reaction increases as well.

It is important to keep in mind that persistent radicals cannot terminate with each other. They may only (reversibly) cross-couple with the growing species, deactivating them. Therefore, in systems where the PRE is present, a pseudo steady state of growing radicals is established through the activation–deactivation process rather than initiation–termination as in conventional radical polymerization.[1,5] In spite of these interesting features, NMP may not be applied to a range of monomers as wide as the other CRP variants. It must also be mentioned that it does not offer the same degree of control over short polymeric chains as can be achieved, for example, in RAFT polymerization.[6]

The most studied and widely used nitroxide is 2,2,6,6-tetramethyl-1-piperidinyl-*N*-oxy (TEMPO). In the presence of excess TEMPO, the equilibrium can become very strongly shifted toward the inactive species significantly reducing polymerization rates. As a result, even though TEMPO can successfully mediate the polymerization of styrene and some of its copolymers, the values of the equilibrium constant are too low for acrylates and several other monomers.[1] Then, TEMPO can only be used for the polymerization of styrene-based monomers at relatively high temperatures (>120 °C).[5]

Other nitroxides such as DEPN (*N*-tert-butyl-*N*-[1-diethylphosphono-(2,2-dimethylpropyl)], also known as SG-1) and TIPNO (1-phenyl-2-methylpropyl-1,1-dimethyl-ethyl-2-nitroxide) can successfully mediate the polymerization of styrene, as well as various other monomers. These derivatives of TEMPO also allow controlling the reaction with a greater proportion of active radicals, which enables lower polymerization temperatures.[1,6]

1.2. Synthesis Control

Although CRP tolerates impurities that would normally end an ionic polymerization, it does not offer such a precise control over polymer molecular structure as ionic polymerization does. In addition, the variation of a single reaction condition could have multiple impacts on chain sequence and overall properties of copolymers. For example, it has been reported that variation in the copolymer composition or in the sequence distribution at the molecular level affects its macroscopic properties.[4,7,8] It becomes evident that a detailed knowledge of the relationship between reaction conditions and copolymer final properties is essential in the design and control of tailor-made materials. It is therefore desirable to gain insight on the influence of operating conditions and process design features on the properties of the material. For this purpose a reliable mathematical model of the process would be very useful.

Articles about modeling of CRcoP processes are relatively scarce. Most of them aim to predict average properties such as composition, conversion, and molecular weights. In this respect, using the method of moments Zhang

and Ray[9,10] modeled several reactors for nitroxide-mediated St homopolymerization and atom transfer radical copolymerization of St and *n*-butyl acrylate, while Ye and Schork[11,12] developed a mathematical model for the copolymerization of St and AMS by NMP in batch and semibatch reactors to determine chain and sequence properties. Wang et al.[2] developed a stochastic model of CRcoP that was used for defining feeding policies appropriate to obtain copolymers with tailor-made molecular structure. On the same path, Wang and Broadbelt[13–15] developed a computational tool based on Monte Carlo stochastic simulations for finding recipes to synthesize copolymers with pre-designed monomer sequences by manipulating the feed profile of the second monomer, the concentration of the unimolecular initiator, and the addition of free nitroxyl radicals.

A feature of copolymer systems is that polymer chains cannot be characterized only by their total chain length. On the contrary, the amount and sequence distribution of both comonomers is required for an appropriate description. This leads to a bivariate MWD, or a copolymer composition-molecular weight distribution (CCD-MWD) and to a sequence length distribution (SLD). A few efforts have been made to model the full bivariate MWD for free-radical copolymerization systems. Papavasiliou and Teymour[16] used a numerical fractionation technique to predict the chain length distribution but they required a pre-specified distribution for its reconstruction. Krallis et al.[17] have developed both a 2D fixed pivot technique and a Monte Carlo algorithm to obtain the distributed molecular properties. The stochastic method proved to be more efficient, easier to implement and less computationally demanding. Soares and Hamielec[18] used Monte Carlo simulations to predict the CCD-MWD along with long chain branching distribution (LCBD) of polyolefins in conventional radical polymerization produced under steady-state conditions with the mechanism of terminal branching. Schütte and Wulkow[19] presented a hybrid deterministic–stochastic method that combines advantages of both approaches. This hybrid method is based on computing the basic chain length distribution deterministically and adding further properties using a stochastic method based on relatively small ensembles of chains. This method was applied for predicting bivariate CCD-MWD and trivariate CCD-MW-LCBDs in copolymerization systems.

To the best of our knowledge, no efforts have been made to obtain the full CCD-MWD in CRcoP systems. Furthermore, temperature effects over the final properties of the material have barely been considered.[9,10] In this context, in this work we develop an advanced mathematical model of the copolymerization of styrene (St) and α-methyl styrene (AMS). The resulting model is then employed to assess the influence of different temperature profiles, feeding policies, and reactor designs on the final product properties, including the full bivariate MWD. The goal of this work is to provide a deeper insight on the influence of operating and design variables on the properties of the final material, and develop a tool capable of aiding in the design of materials tailored for specific applications.

2. Methods

2.1. Mathematical Model

The process under study is the synthesis of poly(St-co-AMS) with BPO (benzoyl peroxide) as initiator and TEMPO as mediator. The most widespread uses of this copolymer are elastomer enhancers, adhesives, and dry inks for photocopiers and laser printers. AMS has also been widely used in free radical co- and terpolymerizations in the surface coatings industry. Besides, it can be employed as an additional control strategy of molecular weight thanks to its low ceiling temperature (64 °C). Above this temperature the effects of depropagation become important enough to cause a decrease in propagation rates and therefore an increase in transfer to monomer. Consequently, small concentrations of AMS in the feed allow lowering molecular weights without the requirement of large amounts of chain transfer agents or initiator.[20,21]

The mathematical model of this process considers the following kinetic mechanism:

$$\text{Initiation}: \quad I \xrightarrow{f\,k_d} 2I^{\circ}, \quad I^{\circ} + M_j \rightarrow R^{j}_{2-j,j-1}, \quad j = 1,2 \tag{1}$$

$$\text{Thermal initiation of St (monomer 1)}: \quad 3M_1 \xrightarrow{k_{th}} R^{1}_{1,0} + R^{1}_{2,0} \tag{2}$$

$$\text{Capping and uncapping}: \; R^{j}_{n_1,n_2} + \text{Te} \underset{k_{uncap,j}}{\overset{k_{cap,j}}{\rightleftharpoons}} D^{j}_{n_1,n_2}, \quad j=1,2 \tag{3}$$

Propagation and depropagation:

$$R^{i}_{n_1,n_2} + M_j \underset{k^{-1}_{p,j}}{\overset{k_{p,ij}}{\rightleftharpoons}} R^{j}_{n_1+2-j,n_2+j-1}, \quad i = 1,2; j = 1,2 \tag{4}$$

Chain termination by coupling:

$$R^{i}_{n_1,n_2} + R^{j}_{s_1,s_2} \xrightarrow{k_{t,ij}} P_{n_1+s_1,n_2+s_2}, \quad i = 1,2; j = 1,2 \tag{5}$$

Chain transfer to monomer:

$$R^{i}_{n_1,n_2} + M_j \xrightarrow{k_{trm,ij}} P_{n_1,n_2} + R^{j}_{2-j,j-1}, \quad i = 1,2; j = 1,2 \tag{6}$$

The chemical species involved are: initiator BPO (I), monomers St (M_1) and AMS (M_2), TEMPO (Te), active radicals ending in monomer j with n_1 units of M_1 and n_2 units of M_2

($R^j_{n_1,n_2}$), dormant (inactive) radicals ending in monomer j with n_1 units of M_1 and n_2 units of M_2 ($D^j_{n_1,n_2}$), and terminated (dead) copolymer chains with n_1 units of M_1 and n_2 units of M_2 (P_{n_1,n_2}). The kinetic parameters were previously obtained by fitting experimental data.[22] Chain termination by disproportionation and disproportionation involving nitroxide were not included since their effects can be neglected.[23] The model takes into account the gel effect by applying the correlation presented by Faliks et al.[24] for CRP of styrene. The dependence of the termination reaction with chain length was neglected. This assumption is equivalent to the use of an average of k_t over all chain lengths, which is a function of temperature only. Even though the dependence of k_t with chain length has been reinvestigated,[25,26] we found good agreement with experimental results without resorting to parameter fitting nor chain length dependent kinetic constants.[22,23] The complexities involved in modeling chain length dependent kinetics seemed therefore unnecessary. The Appendix shows the kinetic constants and model parameters along with the mass balances drawn from the kinetic mechanism for both a tubular reactor with side feeds and a semibatch reactor.

The well-known method of moments with double index was used for modeling the average properties of the copolymer (number-average molecular weight ($\overline{M}_n$), weight-average molecular weight ($\overline{M}_w$), polydispersity index (PDI), global and individual conversion, and instantaneous and global average composition). By means of this method, the mass balances of the polymer species are transformed in order to obtain balances for the first moments of the copolymer MWD, from which the average properties can be computed. The resulting moment balances are shown in the Appendix.

In order to model the SLD, several authors have used methods based on statistical or probabilistic approaches.[27–29] In particular, Monte Carlo methods have been developed that allow analyzing the entire population of chains at various levels of details. In this way, even the explicit sequences of monomers along each chain can be tracked.[13,14,30] The main drawback of these approaches is that their computational cost is usually very high. A different approach involves deterministic models. They are usually based on formulating a parallel kinetic mechanism considering monomer sequences as the reacting species. The information provided by this second method is less exhaustive, because the SLD of the whole resin but not of the individual chains can be modeled, but it is still detailed enough to be able to compare the obtained resins. In this work, we use this second approach, where monomer sequences are understood as chain fragments in any copolymer chain composed by a single monomer. From this kinetic mechanism, mass balances can be deduced for the monomer sequences. It is straightforward to solve the resulting equations due to the short length of the monomer blocks. However, previous works employing this approach have only predicted averages values of the SLD.[11,31–33] In this work, the complete SLD of the copolymers is computed. The kinetic mechanism and sequence mass balances are also shown in the Appendix.

The full bivariate MWD was obtained using 2D probability generating functions (pgf). This technique consists in transforming mass balances of polymeric species, characterized by the number of units of each comonomer, to the 2D pgf domain. In this way balance equations for the 2D pgf transform of the bivariate MWD are obtained. The set of pgf balances is shown in the Appendix.

The full bivariate MWD is recovered from the pgf by applying an appropriate inversion method as reported by Asteasuain and Brandolin.[34]

It is important to point out that the pgf method does not require any a priori knowledge of the shape of the MWD, and can deal with all kinds of complex kinetic mechanisms. Additional information on the pgf method and inversion procedure is given in the Appendix.

The implementation of the models was performed in gPROMS (Process Systems Enterprise, Ltd.) in a standard desktop computer.

2.2. Process Analysis

The effect of different AMS feeding policies and temperature profiles was analyzed theoretically for several reactor types and configurations. We aim at tuning the molecular structure along the copolymer chain through manipulation of the rate of incorporation of comonomers during the growing period of the pseudo living chains. For this purpose tubular and semibatch reactors seem to be ideal because they allow modifying the concentration of the different comonomers by appropriate feeding policies. Even a batch reactor could be appropriate, since spontaneous changes may be obtained due to the different reactivity ratios of the comonomers. In this work, then, we compare the performances of batch, semibatch, and tubular reactors with side feeds, all operating in bulk.

The residence time for all the reactors under study was kept constant in 60 min and equal total amount of reactants. The ratio of initiator and TEMPO used was [BPO]/[TEMPO] = 1.24.

2.2.1. AMS Feeding Policies

The effect of AMS feeding policies on the final product was carried out by splitting the total inlet of this comonomer. The AMS not fed at the beginning of the reaction was added at a constant rate from a given moment up to the final reaction time for the semibatch reactor, or injected into a given lateral feed for the tubular reactor. The

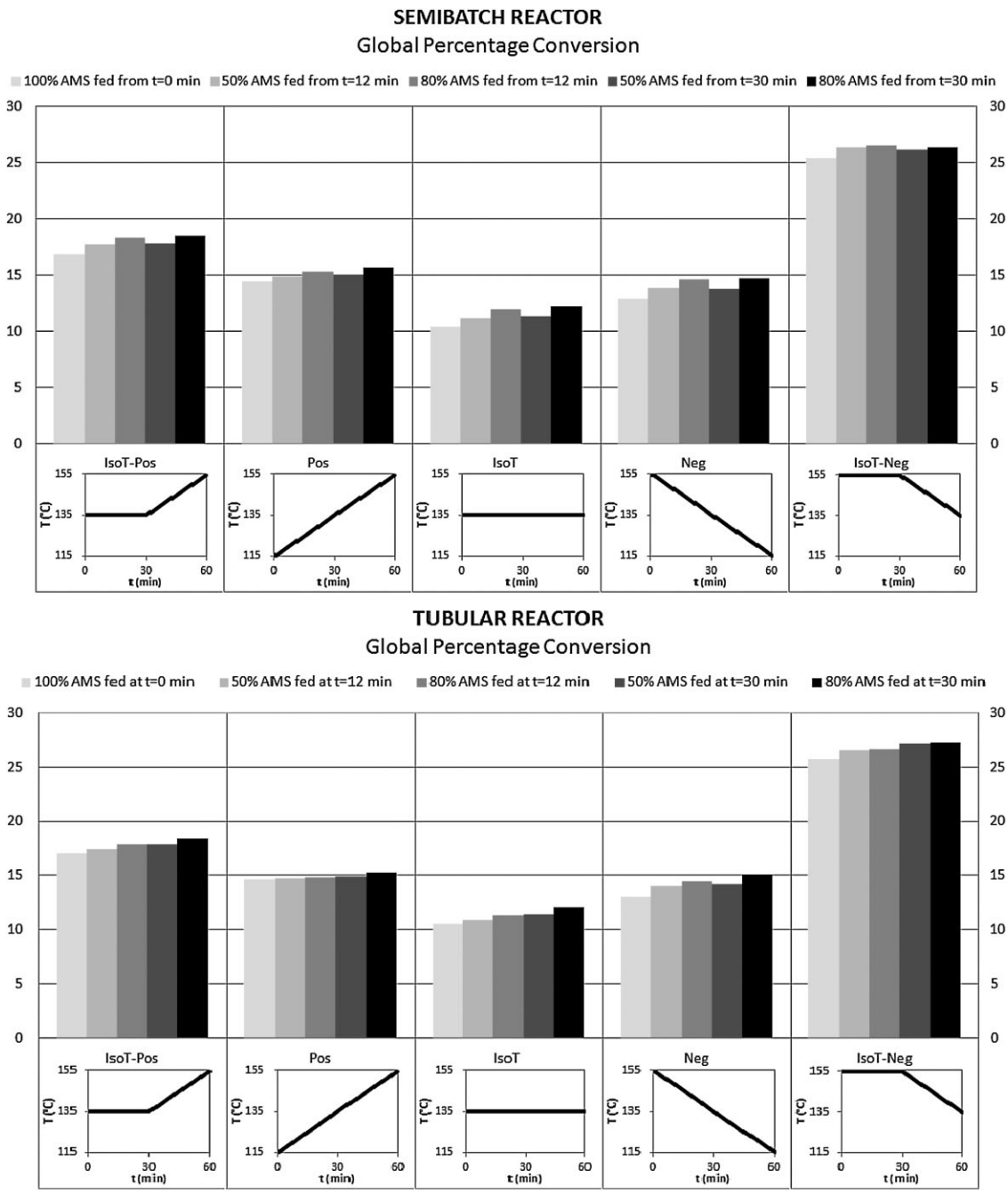

Figure 1. Global conversion for several feeding policies, temperature profiles and reactor designs.

feeding of the remaining reagents (St, TEMPO, and BPO) was performed at time zero (semibatch) or at the reactor inlet (tubular).

2.2.2. Temperature Profiles

The effects of the following temperature profiles were analyzed. From now on the values of time t referred to the tubular reactor should be understood as mean residence times:

Profile 1: *Isothermal* (“*IsoT*”)

$$T = T_0 \tag{7}$$

The temperature used was 135 °C.

Profile 2: *Increasing temperature with constant slope* (“*Pos*”).

$$T = T_0 + kt \tag{8}$$

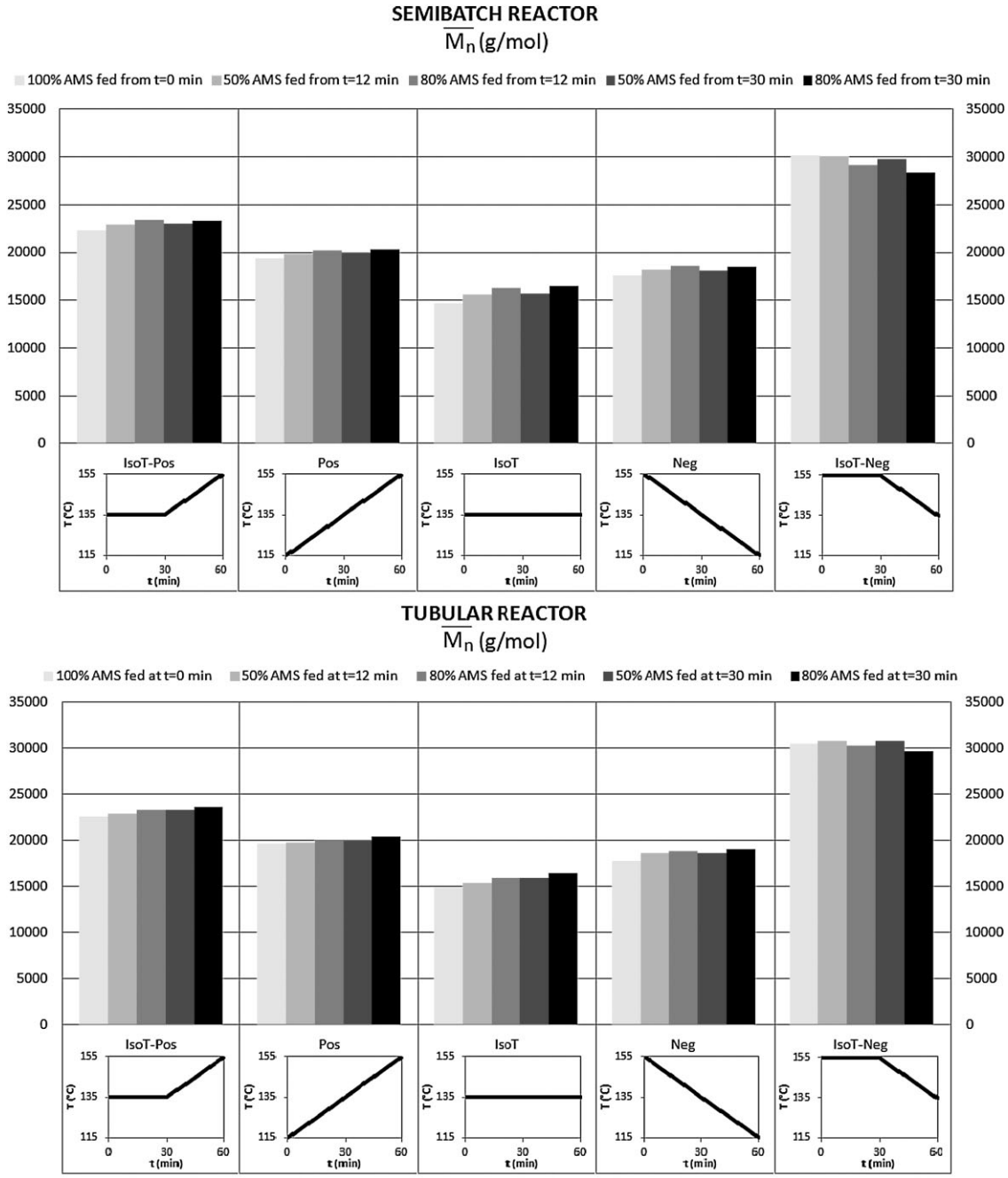

Figure 2. Number average molecular weights for several feeding policies, temperature profiles and reactor designs.

with $T_0 = 110\,^{\circ}\mathrm{C}$ and $k = 2/3\,^{\circ}\mathrm{C} \cdot \mathrm{min}^{-1}$.

Profile 3: *Decreasing temperature with constant slope* (*"Neg"*).

$$T = T_0 - k\,t \tag{9}$$

with $T_0 = 155\,^{\circ}\mathrm{C}$ and $k = 2/3\,^{\circ}\mathrm{C} \cdot \mathrm{min}^{-1}$.

Profile 4: *Isothermal until $t = 30$ min + steady increase in T* (*"IsoT-Pos"*)

The temperature was kept fixed at 135 °C for 30 min and then increased with a constant slope of $2/3\,^{\circ}\mathrm{C} \cdot \mathrm{min}^{-1}$.

Profile 5: *Isothermal until $t = 30$ min + steady decrease in T* (*"IsoT-Neg"*).

The temperature was kept fixed at 155 °C for 30 min and then decreased with a constant slope of $2/3\,^{\circ}\mathrm{C} \cdot \mathrm{min}^{-1}$.

The profiles were selected to cover a wide range of conditions that could be used to produce useful resins. Given that the studied synthesis is a bulk polymerization,

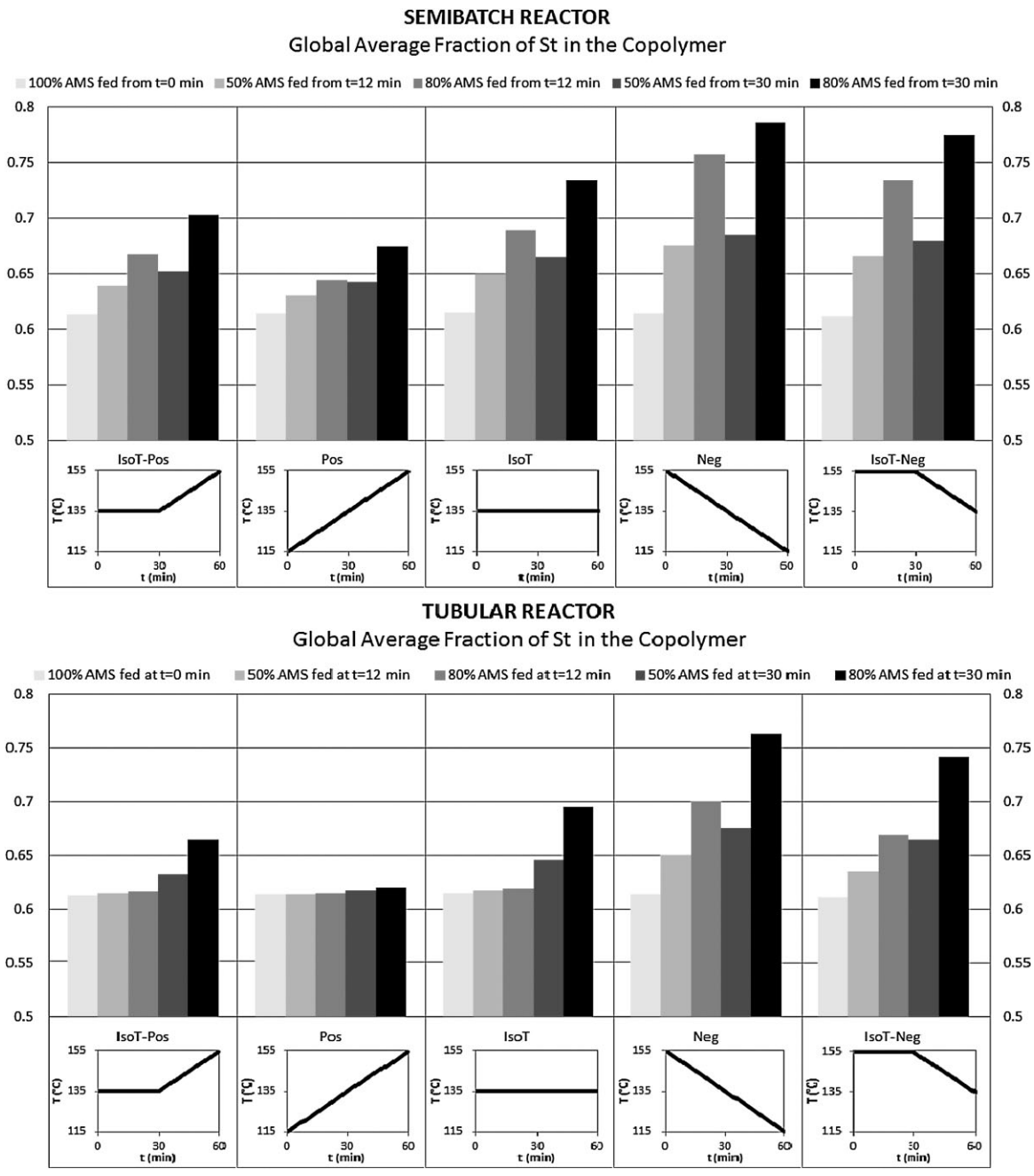

Figure 3. Global average fraction of St in the copolymer for several feeding policies, temperature profiles, and reactor designs.

temperature should not surpass 155 °C to avoid fast reaction rates that would lead to undesirably high molecular weight material and excessive viscosity problems.

An objective of this paper is studying not only how to obtain a specified resin by manipulating the thermal profile but also to help understanding how the thermal profile causes variations in the copolymer properties.

3. Results and Discussion

3.1. Effects on Conversion and Molecular Weight

For the conditions used in this work, conversion increases with temperature and shows little variation with the feeding policies and reactor configuration (Figure 1). Propagation rates are favored at high temperatures as well

as the equilibrium constant of the capping/uncapping reaction. This results in longer periods of activation, which then allows the chains to incorporate more monomer units. Conversions of up to 28% can be achieved with the "*IsoT-Neg*" temperature profile, while only around 11% is obtained with the isothermal operation at 135 °C.

When lower percentages of AMS are fed at the beginning of the reaction time, the general trend observed is an increase in conversion. This is thought to be caused by the reduction of the AMS depropagation effect due to its lower concentration.

Similar trends are observed for the copolymer $\overline{M}_n$ for the different operating policies, as is shown in Figure 2. This indicates that the molecular weight development is mainly ruled by conversion, with little influence of the distribution of the AMS feed.

3.2. Effects on Copolymer Composition

It may be observed in Figure 3 that significant changes occur in copolymer composition by changing feeding policies, temperatures, or reactor designs. In the cases where all the reactants are fed at the reactor inlet/charged at initial reaction time, the different temperature profiles do not affect the copolymer composition. This happens because composition is determined by reactivity ratios, which are considered to be independent of temperature in the temperature range analyzed. However, copolymer composition can be tuned by means of the combination of the AMS feeding and temperature profile. In general, deriving higher proportions of AMS to additional feeds at later conversions leads to a higher content of St, due to the initial St-rich chains. The temperature profile after the AMS feeding point plays an important role, too. For instance, the 80% AMS fed at $t = 30$ min with temperature profile "*IsoT-Neg*" leads to a higher AMS incorporation than the same feeding policy with the "*Pos*" profile. This is because the higher temperature level in the "*IsoT-Neg*" allows the reaction to proceed up to a higher extent, resulting in longer, AMS richer segments.

For the operating policies studied in this work, the average copolymer composition obtained in the semibatch reactor appears to be more sensitive to policy changes, a characteristic that would give it greater flexibility for producing different resin grades.

Figure 4 shows the instantaneous copolymer composition for the isothermal operation. It is important to note that the composition distribution along the chain differs significantly for the different feeding policies. For the tubular reactor the chains are composed by two distinguishable different blocks. The first one is richer in St. The proportion of St in the St-rich end increases as more AMS is derived toward the end of the reactor. A similar analysis can be performed for the semibatch reactor. In this case,

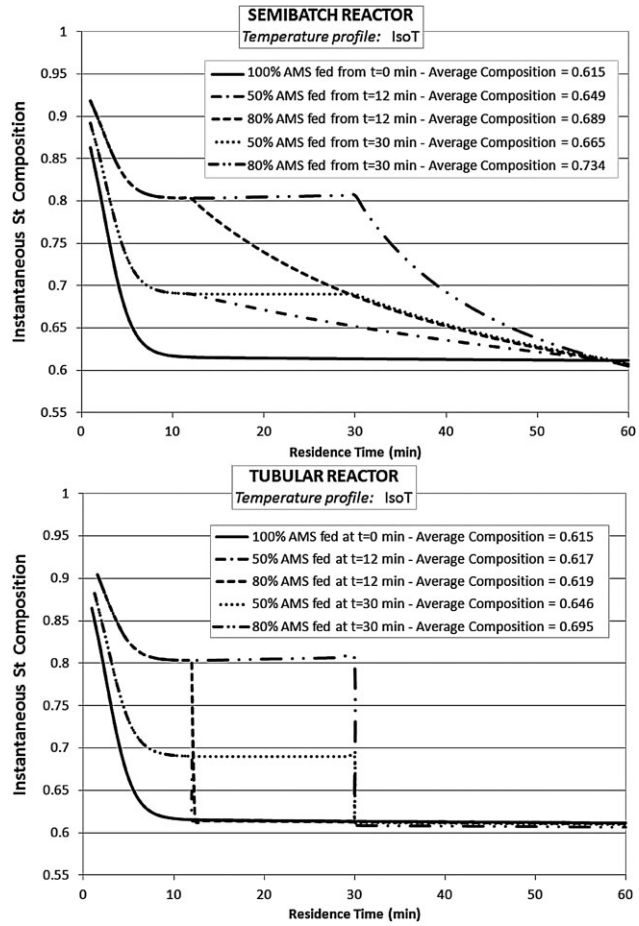

Figure 4. Instantaneous average fraction of St in the copolymer being formed for different feeding policies and reactor designs for isothermal temperature profile.

however, changes in the chain composition are gradual, resulting in gradient copolymers. The different temperature profiles do not cause especially remarkable changes in instantaneous composition profiles for any of the studied feeding policies. However, the temperature profiles affect the conversion level, so the final global compositions do change. These results illustrate the flexibility of the reactor configurations and operating conditions for achieving different molecular structures, and the usefulness of the mathematical model for analyzing the different process designs.

As an example of the capabilities of our theoretical model, full bivariate MWDs for two different temperature profiles and the same reactor design and feeding policy are shown in Figure 5. For each case we show a contour plot of the distribution where, as an interpretation aid, lines of constant composition are included. The differences in molecular weight, and in particular composition distribution, can be appreciated. It may be seen in the figure that

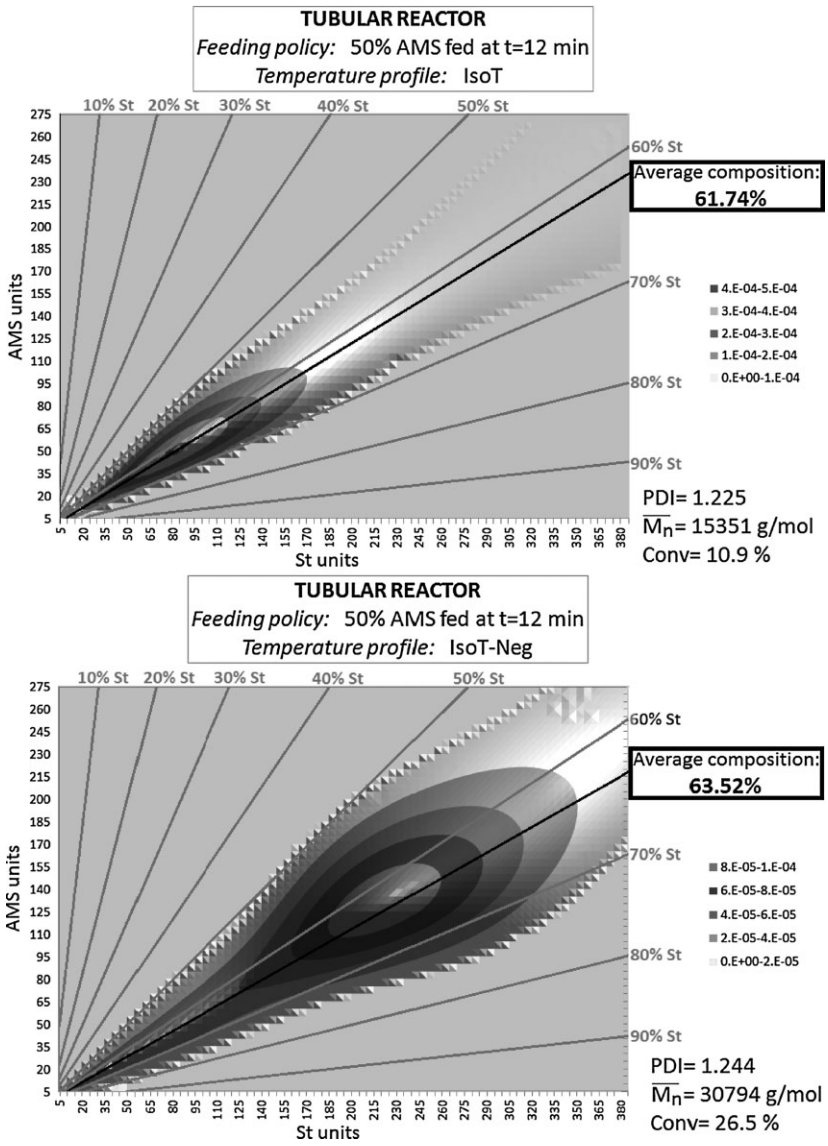

Figure 5. Contour plots and lines of constant composition for a particular feeding policy and reactor design and two different temperature profiles.

even though the average St content is similar, the CCD is broader when using the "*IsoT-Neg*" profile.

3.3. Effects on the St Sequence Length Distribution (SLD)

The level of depropagation of AMS causes the blocks of this comonomer in the product chains to be all of unitary length. Moreover, the length of St sequences is also small.

Figure 6 illustrates the St SLD in the final copolymer for the isothermal operation. Continuous lines have been used to connect the discrete points of the distribution to facilitate the interpretation. It can be seen that decreasing the initial concentration of AMS in the semibatch reactor allows production of a copolymer with a greater proportion of sequences with more than one St unit. The effect of the feeding policies on the SLD is less marked for the tubular reactor.

We have verified that using different temperature profiles also influences the St SLD. It is possible to reduce the proportion of unitary length St sequences by operating at higher temperatures, together with higher concentrations of St.

3.4. About the "Livingness" of the Reaction

In all the cases studied in this work the PDI ranges from 1.19 to 1.27, well below the usual value of 1.5 for free radical polymerizations with termination by combination. Since this is a measure of polymer uniformity, these low values would suggest that the majority of the chains are active and growing at the same speed on average, even when the temperature remains at 155 °C for an extended period of time. However, deeper analysis of simulation outcomes shows that this is not always the case. The model provides extra information that can help to quantify how "alive" the reaction really is.

A true "living" polymerization should show a linear dependence of number average molecular weight with conversion. In the reactions studied in this work, the relationship between $\overline{M}_n$ and conversion is not perfectly linear, but the deviation is slight. As an example we show in Figure 7 two $\overline{M}_n$ versus conversion lines for a tubular reactor with 50% AMS fed at 12 min and different temperature profiles. Please note that the conversion diminishes abruptly at the injection point, since the added monomer dilutes the reacting medium. This is only observable in the curve that corresponds to the faster reaction; in the slower one the conversion at 12 min was $<0.5\%$.

The analysis of the full bivariate MWD and of the fraction of terminated copolymer chains shows that high temperature favors the termination reactions. Since terminated chains cannot grow any further, when significant termination occurs prematurely the material loses uniformity. In our simulations, the percentage of terminated chains generally remains around 10%, which can be seen as a

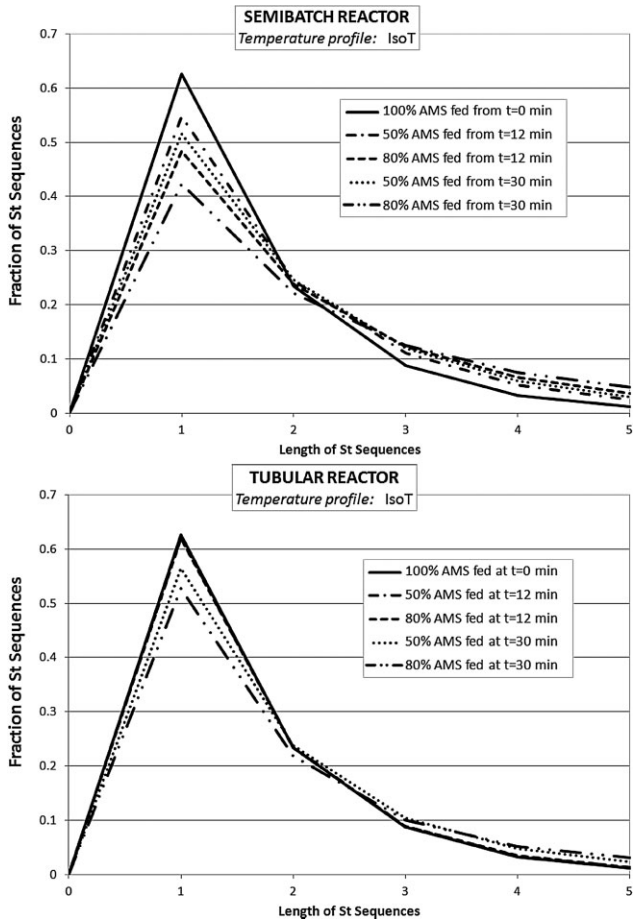

Figure 6. Fraction of St sequences of different length for different feeding policies and reactor designs for the isothermal temperature profile.

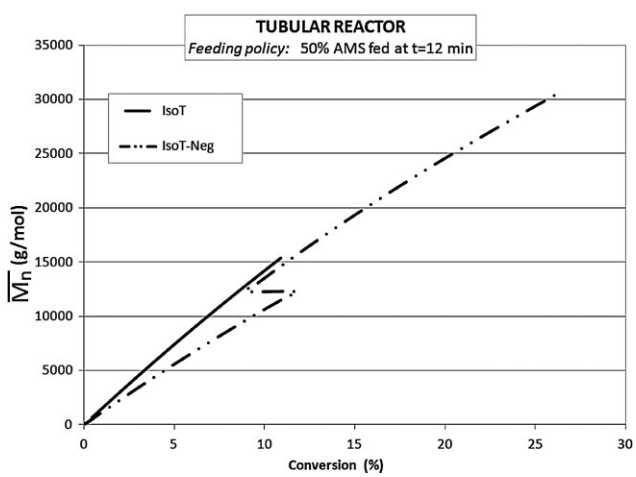

Figure 7. Evolution of number average molecular weight with conversion.

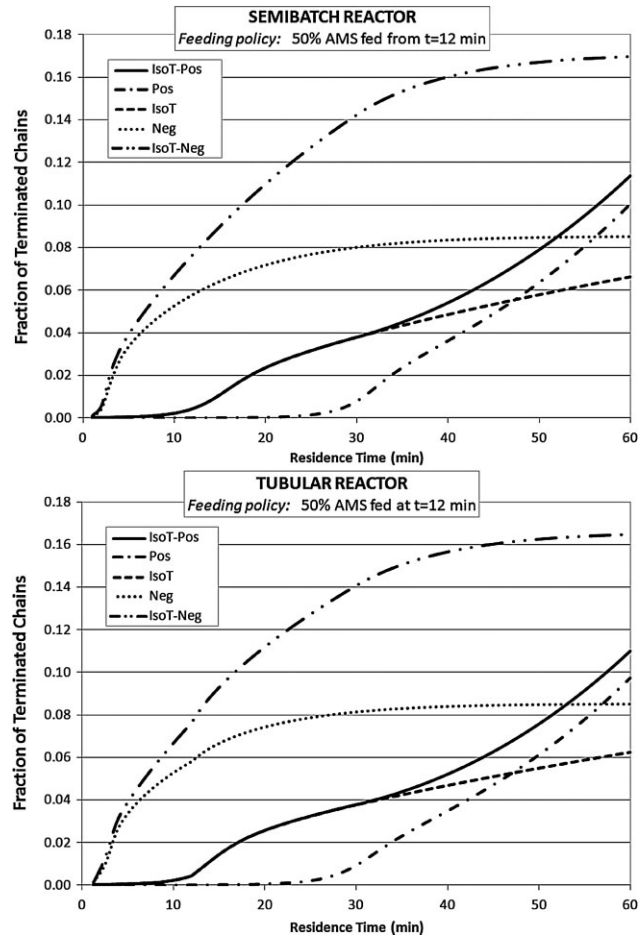

Figure 8. Fraction of terminated chains in the reacting medium for different temperature profiles and reactor designs for the same feeding policy (50% AMS fed at/from $t = 12$ min).

favorable value. However, for the "*IsoT-Neg*" temperature profile this percentage can surpass 16% (Figure 8). Although higher conversion and molecular weights can be achieved when operating at high temperatures, it can be easily observed that the fraction of terminated chains rapidly increases under those conditions.

The bivariate MWD reveals that when the temperature remained at 155 °C for half the total residence time an important fraction of terminated chains is obtained. For all feeding policies and reactor configurations, the MWD of the "*IsoT-Neg*" profile shows a flat shape in the low molecular weight region and a peak at higher molecular weights. We show a representative example in Figure 9, where the MWD resulting from two different temperature profiles on a tubular reactor may be compared. The results are strikingly different. For the "*IsoT*" profile, the MWD is symmetric and shows no special features in the low molecular weight region. For the "*IsoT-Neg*" profile, on the other hand, a flat region appears at the low molecular weight region that has

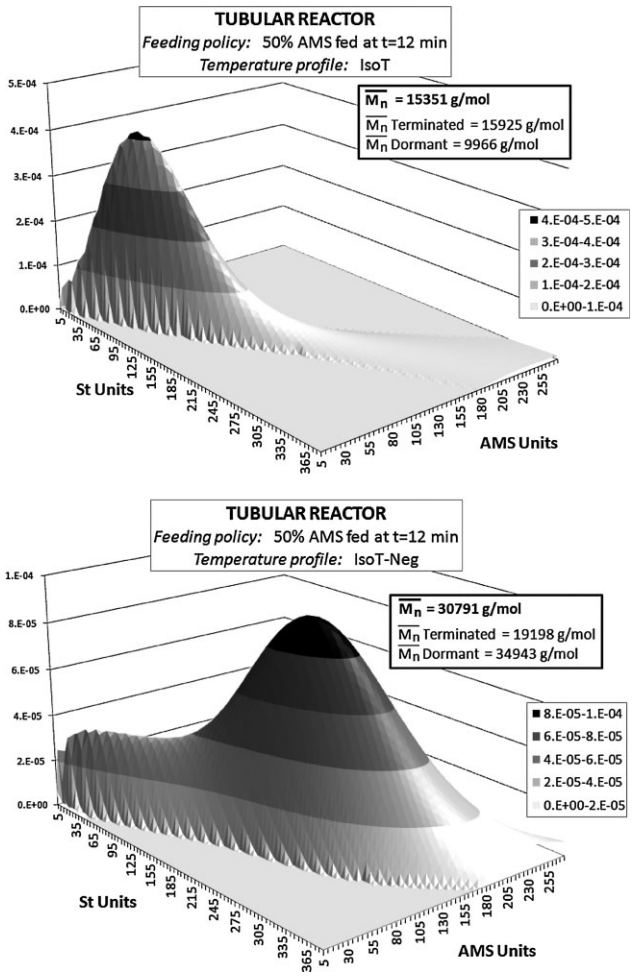

Figure 9. Overall copolymer full MWD for tubular reactor and two temperature profiles (''*IsoT*'' and ''*IsoT-Neg*'') for the same feeding policy (50% AMS fed at $t = 12$ min).

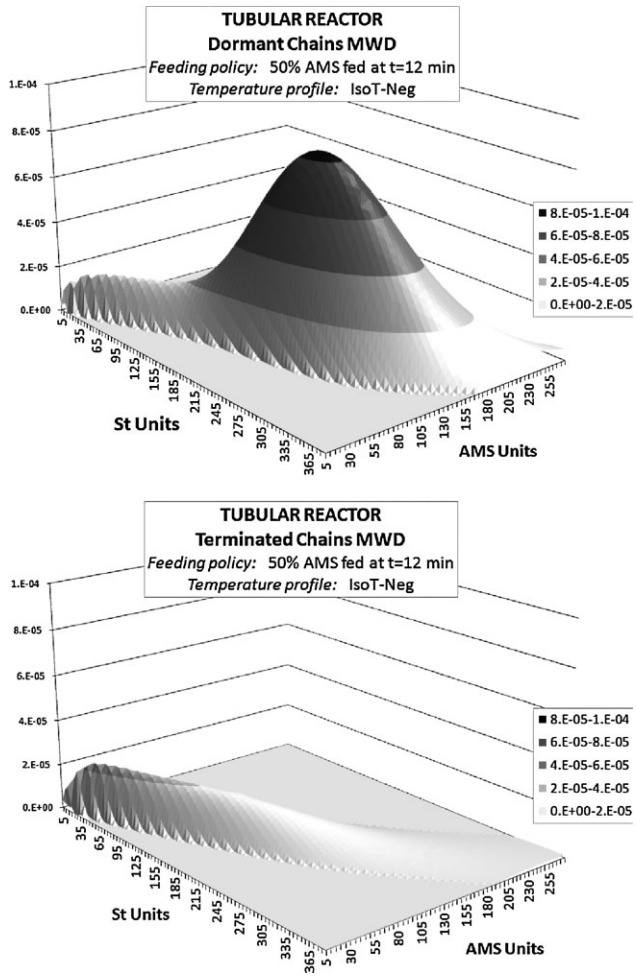

Figure 10. Dormant and terminated copolymer MWD for tubular reactor, ''*IsoT-Neg*'' temperature profile and 50% AMS fed at $t = 12$ min.

a barely noticeable peak located approximately at the average molecular weight of terminated chains. The MWD peak is positioned at the average molecular weight of dormant species. The final average molecular weight of the overall copolymer is between these two values. Furthermore, the overall copolymer MWD can be separated into two MWD corresponding to the dormant species and the terminated chains (Figure 10).

In summary, the smaller the fraction of terminated chains, the closer the $\overline{M}_n$ of the overall copolymer is to the one corresponding to the dormant species and the greater the ''livingness'' of the reaction.

4. Conclusion

The copolymerization of St and AMS by NMP has been successfully modeled for different reactors. The model predictions include the full CCD-MWD and the effect of temperature on the final properties of the material, two aspects that so far have had little or no treatment in the literature for CRcoP systems. The results are helpful to select the process and design conditions best suited to produce a material with given required characteristics. Moreover, given that it is a common issue in all polymerizations to have slight to severe cases of uncontrolled temperature it is useful to evaluate how this can affect the copolymer properties. Proper knowledge of this matter could make the most of everyday production, enabling the finding of appropriate uses for each resin and therefore reducing out of specification product to a minimum.

Both a higher temperature and the distributed feeding of AMS favor higher molecular weights and larger St contents in the final copolymer obtained.

The population of dead chains remains low even when operating at high temperatures, as long as that temperature

level is not maintained for a long period of time. In this sense, the model proved to be a useful tool to adequately characterize the material being produced. The simulation of average properties only has proven to be insufficient to determine in detail the molecular structure of copolymers.

The model predicts that St sequences are mostly short, while the AMS sequences are all unitary. By distributing the feeding of AMS or increasing the temperature, the copolymer gets richer in St, with longer blocks of this monomer.

Semibatch reactors seem to be more suitable for the production of high value-added resins given its higher flexibility: variations in operating conditions or design features allow obtaining a broader spectrum of copolymer compositions and molecular structures than their tubular counterparts. However, tubular reactors are more advantageous not only for large scale production but also because they have proved to be less sensitive to out of range temperature.

On the other hand the ability to manipulate the temperature profiles greatly expands the flexibility of both types of reactors since it allows increasing the product portfolio. Moreover, given this information it is possible to adapt the design of reactors (including those already built) to produce different resins.

Additionally, even though this model has been developed for the study of St-AMS NMP, it can be generalized to include many types of living radical polymerization and comonomer pairs.

Finally, the model provides detailed information on the copolymer molecular structure depending on the design and operating conditions, which is especially useful for process operation. This makes it a valuable predictive tool that would anticipate the final properties of the material before any change occurs in the operating regime. It also has great potential as an optimization tool that would aid in the production of tailor-made copolymers.

Appendix A: Balance Equations

Semibatch reactor

$$\frac{\mathrm{d}(\rho_{\mathrm{mix}}\cdot V)}{\mathrm{d}t} = F_{\mathrm{sb,lat}} \tag{A1}$$

Mass balances of reacting species

$$\frac{\mathrm{d}([j]\cdot V)}{\mathrm{d}t} = X_j\cdot V + \frac{F_{\mathrm{sb,lat}}\cdot x_{j,\mathrm{lat}}}{\mathrm{MW}_j} \quad j = I, M_1, M_2, Te \tag{A2}$$

Balances of moments, pgfs and monomer sequences:

$$\begin{aligned}\frac{\mathrm{d}(\chi\cdot V)}{\mathrm{d}t} = X_\chi\cdot V \quad \chi = \lambda^j_{a,b}, \mu^j_{a,b}, \varepsilon^j_{a,b}, \left[\lambda^j_{a,b}\sigma^j_{a,b}(z_1,z_2)\right], \left[\mu^j_{a,b}\varphi^j_{a,b}(z_1,z_2)\right],\\ \left[\varepsilon^j_{a,b}\vartheta^j_{a,b}(z_1,z_2)\right], SD^j_n, SR^j_n, SP^j_n, \lambda s^j_{a,b}, \mu s^j_{a,b}, \varepsilon s^j_{a,b}\end{aligned} \tag{A3}$$

Tubular reactor

Global mass balance

$$\frac{\mathrm{d}(\rho_{\mathrm{mix}}\cdot v)}{\mathrm{d}z} = F_{\mathrm{tub,lat}} \tag{A4}$$

Variable $F_{\mathrm{tub,lat}}$ is a flux per unit length that is used to approximate the point mass inlet to the tubular reactor at a side position. This variable is non-zero only in a very short length interval Δz starting at the injection point. $F_{\mathrm{tub,lat}}$ is calculated as

$$AF_{\mathrm{tub,lat}}\Delta z = \text{side feed mass flow} \tag{A5}$$

where A is the reactor cross-sectional area and Δz is the length interval in which $F_{\mathrm{tub,lat}}$ is non-zero.

Mass balances of reacting species

$$\frac{\mathrm{d}([j]\cdot v)}{\mathrm{d}z} = X_j + \frac{F_{\mathrm{tub,lat}}\cdot x_{j,\mathrm{lat}}}{\mathrm{MW}_j} \quad j = I, M_1, M_2, Te \tag{A6}$$

Balances of moments, pgfs, monomer sequences, and their moments:

$$\frac{d(\chi\cdot v)}{dz} = X_\chi \quad \chi = \lambda^j_{a,b}, \mu^j_{a,b}, \varepsilon^j_{a,b}, \left[\lambda^j_{a,b}\sigma^j_{a,b}(z_1,z_2)\right], \left[\mu^j_{a,b}\varphi^j_{a,b}(z_1,z_2)\right], \left[\varepsilon^j_{a,b}\vartheta^j_{a,b}(z_1,z_2)\right], SD^j_n, SR^j_n, SP^j_n, \lambda s^j_{a,b}, \mu s^j_{a,b}, \varepsilon s^j_{a,b} \quad \text{(A7)}$$

Reaction rates

Initiator

$$X_{\mathrm{I}} = -k_{\mathrm{d}}[\mathrm{I}] \quad \text{(A8)}$$

TEMPO

$$X_{\mathrm{Te}} = -k_{\mathrm{cap},1}[\mathrm{Te}]\lambda^1_{0,0} + k_{\mathrm{uncap},1}\mu^1_{0,0} - k_{\mathrm{cap},2}[\mathrm{Te}]\lambda^2_{0,0} + k_{\mathrm{uncap},2}\mu^2_{0,0} \quad \text{(A9)}$$

Monomer j ($j = 1$: styrene, $j = 2$: α-methylstyrene)

$$X_j = -2fk_{\mathrm{d}}[\mathrm{I}]\left(\frac{[\mathrm{M}_j]}{[\mathrm{M}_1]+[\mathrm{M}_2]}\right) - 3k_{\mathrm{th}}[\mathrm{M}_j]^3\delta_{j,1} - \left(k_{\mathrm{p},1j} + k_{\mathrm{trm},1j}\right)[\mathrm{M}_j]\lambda^1_{0,0} - \left(k_{\mathrm{p},2j} + k_{\mathrm{trm},2j}\right)[\mathrm{M}_j]\lambda^2_{0,0} + k^{-1}_{\mathrm{p},j}p_{22}\lambda^j_{0,0}\,\delta_{j,2} \quad \text{(A10)}$$

Dormant copolymer with n_1 units of monomer 1 and n_2 units of monomer 2 with a monomer j final unit

$$X_{\mathrm{D}^j_{n_1,n_2}} = k_{\mathrm{cap},j}[\mathrm{Te}]\left[\mathrm{R}^j_{n_1,n_2}\right] - k_{\mathrm{uncap},j}\left[\mathrm{D}^j_{n_1,n_2}\right] \quad \text{(A11)}$$

Macroradical with n_1 units of monomer 1 and n_2 units of monomer 2 with a monomer j final unit

$$\begin{aligned} X_{\mathrm{R}^j_{n_1,n_2}} = & \left\{2fk_{\mathrm{d}}[\mathrm{I}]\left(\frac{[\mathrm{M}_j]}{[\mathrm{M}_1]+[\mathrm{M}_2]}\right) + \left(k_{\mathrm{trm},jj}\lambda^j_{0,0} + k_{\mathrm{trm},ij}\lambda^i_{0,0}\right)[\mathrm{M}_j]\right\}\delta_{n_1,1\delta_{j,1}}\delta_{n_2,1\delta_{j,2}} \\ & + \left(\tfrac{1}{2}\right)k_{\mathrm{th}}[\mathrm{M}_j]^3\left(\delta_{n_1,1}\delta_{n_2,0} + \delta_{n_1,2}\delta_{n_2,0}\right)\delta_{j,1} + k_{\mathrm{p},ij}[\mathrm{M}_j]\left[R^i_{n_1-1\delta_{j,1},n_2-1\delta_{j,2}}\right] \\ & + k^{-1}_{\mathrm{p},j}p_{22}\left[\mathrm{R}^j_{n_1,n_2+1}\right]\delta_{j,2} + k_{\mathrm{p},jj}[\mathrm{M}_j]\left[\mathrm{R}^j_{n_1-1\delta_{j,1},n_2-1\delta_{j,2}}\right] + k_{\mathrm{uncap},j}\left[\mathrm{D}^j_{n_1,n_2}\right] \\ & - \left\{\begin{array}{l} k_{\mathrm{cap},j}[\mathrm{Te}] + \left(k_{\mathrm{p},jj} + k_{\mathrm{trm},jj}\right)[\mathrm{M}_j] \\ + \left(k_{\mathrm{p},ji} + k_{\mathrm{trm},ji}\right)[\mathrm{M}_i] + k_{\mathrm{t},jj}\lambda^j_{0,0} + k_{\mathrm{t},ji}\lambda^i_{0,0} \end{array}\right\}\left[\mathrm{R}^j_{n_1,n_2}\right] \end{aligned} \quad \text{(A12)}$$

Dead copolymer with n_1 units of monomer 1 and n_2 units of monomer 2

$$\begin{aligned} X_{\mathrm{P}_{n_1,n_2}} = & \left(k_{\mathrm{trm},11}[\mathrm{M}_1] + k_{\mathrm{trm},12}[\mathrm{M}_2]\right)\left[\mathrm{R}^1_{n_1,n_2}\right] + \left(k_{\mathrm{trm},21}[\mathrm{M}_1] + k_{\mathrm{trm},22}[\mathrm{M}_2]\right)\left[\mathrm{R}^2_{n_1,n_2}\right] \\ & + k_{\mathrm{t},12}\sum_{l=0}^{n_1-l}\sum_{r=0}^{n_2-r}\left[\mathrm{R}^1_{n_1-l,n_2-r}\right]\left[\mathrm{R}^2_{l,r}\right] + \left(\tfrac{1}{2}\right)k_{\mathrm{t},11}\sum_{l=0}^{n_1-l}\sum_{r=0}^{n_2-r}\left[\mathrm{R}^1_{n_1-l,n_2-r}\right]\left[\mathrm{R}^1_{l,r}\right] \\ & + \left(\tfrac{1}{2}\right)k_{\mathrm{t},22}\sum_{l=0}^{n_1-l}\sum_{r=0}^{n_2-r}\left[\mathrm{R}^2_{n_1-l,n_2-r}\right]\left[\mathrm{R}^2_{l,r}\right] \end{aligned} \quad \text{(A13)}$$

ath, bth order moments of the dormant chains with a monomer j final unit ($a = 0,1,2$, $b = 0,1,2$)

$$X_{\mu^j_{a,b}} = k_{\mathrm{cap},j}[\mathrm{Te}]\lambda^j_{a,b} - k_{\mathrm{uncap},j}\mu^j_{a,b} \quad \text{(A14)}$$

ath, bth order moments of the macroradical with a monomer j final unit ($a = 0,1,2$, $b = 0,1,2$)

$$\begin{aligned} X_{\lambda^j_{a,b}} = & \left\{ 2fk_{\mathrm{d}}[\mathrm{I}]\left(\frac{[\mathrm{M}_j]}{[\mathrm{M}_1]+[\mathrm{M}_2]}\right) + \left(k_{\mathrm{trm},1j}\lambda^1_{0,0} + k_{\mathrm{trm},2j}\lambda^2_{0,0}\right)[\mathrm{M}_j] \right\}\left(1^a 0^b \delta_{j,1} + 0^a 1^b \delta_{j,2}\right) \\ & + k_{\mathrm{th}}[\mathrm{M}_j]^3\left(1^a 0^b + 2^a 0^b\right)\delta_{j,1} + k_{\mathrm{uncap},j}\mu^j_{a,b} + k^{-1}_{\mathrm{p},j}p_{22}\sum_{g=0}^{b}\binom{b}{g}(-1)^g\lambda^j_{a,b-g}\delta_{j,2} \\ & + k_{\mathrm{p},1j}[\mathrm{M}_j]\left\{\left(\sum_{h=0}^{a}\binom{a}{h}\lambda^1_{a-h,b}\right)\delta_{j,1} + \left(\sum_{g=0}^{b}\binom{b}{g}\lambda^1_{a,b-g}\right)\delta_{j,2}\right\} \\ & + k_{\mathrm{p},2j}[\mathrm{M}_j]\left\{\left(\sum_{h=0}^{a}\binom{a}{h}\lambda^2_{a-h,b}\right)\delta_{j,1} + \left(\sum_{g=0}^{b}\binom{b}{g}\lambda^2_{a,b-g}\right)\delta_{j,2}\right\} \\ & - \left\{ \begin{array}{l} k_{\mathrm{cap},j}[\mathrm{Te}] + \left(k_{\mathrm{p},1j} + k_{\mathrm{trm},1j}\right)[\mathrm{M}_1] + \left(k_{\mathrm{p},2j} + k_{\mathrm{trm},2j}\right)[\mathrm{M}_2] + \\ k_{\mathrm{t},j1}\lambda^1_{0,0} + k_{\mathrm{t},j2}\lambda^2_{0,0} + k^{-1}_{\mathrm{p},j}p_{22}\,\delta_{j,2} \end{array} \right\}\lambda^j_{a,b} \end{aligned} \tag{A15}$$

ath, bth order moments of the dead copolymer ($a = 0,1,2$, $b = 0,1,2$)

$$\begin{aligned} X_{\varepsilon_{a,b}} = & \left(k_{\mathrm{trm},11}[\mathrm{M}_1] + k_{\mathrm{trm},12}[\mathrm{M}_2]\right)\lambda^1_{a,b} + \left(k_{\mathrm{trm},21}[\mathrm{M}_1] + k_{\mathrm{trm},22}[\mathrm{M}_2]\right)\lambda^2_{a,b} \\ & + k_{\mathrm{t},12}\sum_{j=0}^{a}\sum_{g=0}^{b}\binom{a}{j}\binom{b}{g}\lambda^1_{a-j,b-g}\,\lambda^2_{j,g} + \left(\tfrac{1}{2}\right)k_{\mathrm{t},11}\sum_{j=0}^{a}\sum_{g=0}^{b}\binom{a}{j}\binom{b}{g}\lambda^1_{a-j,b-g}\,\lambda^1_{j,g} \\ & + \left(\tfrac{1}{2}\right)k_{\mathrm{t},22}\sum_{j=0}^{a}\sum_{g=0}^{b}\binom{a}{j}\binom{b}{g}\lambda^2_{a-j,b-g}\,\lambda^2_{j,g} \end{aligned} \tag{A16}$$

Appendix B: Kinetic Mechanism for Monomer Sequences and Sequences Reaction Rates

$$\text{Initiation}: \quad I \xrightarrow{f\,k_{\mathrm{d}}} 2I^{\circ},\ I^{\circ} + M_j \rightarrow \mathrm{SR}^j_{2-j,j-1}, \quad j = 1,2 \tag{B1}$$

$$\text{Thermal Initiation of St (monomer 1)}: \quad 3\,M_1 \xrightarrow{k_{\mathrm{th}}} \mathrm{SR}^1_{1,0} + \mathrm{SR}^1_{2,0} \tag{B2}$$

$$\text{Capping and Uncapping}: \quad \mathrm{SR}^j_n + \mathrm{Te} \underset{k_{\mathrm{uncap},j}}{\overset{k_{\mathrm{cap},j}}{\rightleftharpoons}} \mathrm{SD}^j_n, \quad j = 1,2 \tag{B3}$$

$$\text{Propagation and Depropagation}: \quad \mathrm{SR}^j_n + M_j \underset{k^{-1}_{\mathrm{p},j}}{\overset{k_{\mathrm{p},jj}}{\rightleftharpoons}} \mathrm{SR}^j_{n+1}, \quad j = 1,2 \tag{B4}$$

$$\mathrm{SR}^i_n + M_j \xrightarrow{k_{\mathrm{p},ij}} \mathrm{SP}^i_n + \mathrm{SR}^j_1, \quad i = \left((2-j)\delta_{j,1} + (j-1)\delta_{j,2}\right); j = 1,2 \tag{B5}$$

$$\text{Chain Termination by Coupling}: \quad \mathrm{SR}^j_n + \mathrm{SR}^j_s \xrightarrow{k_{\mathrm{t},jj}} \mathrm{SP}^j_{n+s}, \quad j = 1,2 \tag{B6}$$

$$\mathrm{SR}^i_n + \mathrm{SR}^j_s \xrightarrow{k_{\mathrm{t},ij}} \mathrm{SP}^i_n + \mathrm{SP}^j_s, \quad i = \left((2-j)\delta_{j,1} + (j-1)\delta_{j,2}\right), j = 1,2 \tag{B7}$$

$$\text{Chain Transfer to monomer}: \quad \mathrm{SR}^i_n + M_j \xrightarrow{k_{\mathrm{trm},ij}} \mathrm{SP}^i_n + \mathrm{SR}^j_1, \quad i = 1,2; j = 1,2 \tag{B8}$$

Sequence of n units of monomer j ending in a capped radical center

$$X_{\mathrm{SD}^j_n} = k_{\mathrm{cap},j}[\mathrm{Te}]\left[\mathrm{SR}^j_n\right] - k_{\mathrm{uncap},j}\left[\mathrm{SD}^j_n\right] \tag{B9}$$

Sequence of n units of monomer j ending in an active radical center

$$\begin{aligned} X_{\mathrm{SR}_n^j} = & \left\{ 2fk_{\mathrm{d}}[\mathrm{I}]\left(\frac{[\mathrm{M}_j]}{[\mathrm{M}_1]+[\mathrm{M}_2]}\right) + \begin{pmatrix} k_{\mathrm{trm},1j}\lambda s_0^1 + k_{\mathrm{trm},2j}\lambda s_0^2 + \\ k_{\mathrm{p},\left((2-j)\delta_{j,1}+(j-1)\delta_{j,2}\right)j}\lambda s_0^{\left((2-j)\delta_{j,1}+(j-1)\delta_{j,2}\right)} \end{pmatrix} [\mathrm{M}_j] \right\}\delta_{n,1} \\ & + k_{\mathrm{th}}[\mathrm{M}_j]^3(\delta_{n,1}+\delta_{n,2})\delta_{j,1} + k_{\mathrm{p},jj}[\mathrm{M}_j]\left[\mathrm{SR}_{n-1}^j\right](1-\delta_{n,1}) \\ & + k_{\mathrm{p},j}^{-1}\left\{\left[\mathrm{SR}_{n+1}^j\right] - \left[\mathrm{SR}_n^j\right](1-\delta_{n,1})\right\}\delta_{j,2} + k_{\mathrm{uncap},j}\left[\mathrm{SD}_n^j\right] \\ & - \left\{ \begin{array}{l} k_{\mathrm{cap},j}[\mathrm{Te}] + (k_{\mathrm{p},j1}+k_{\mathrm{trm},j1})[\mathrm{M}_1] \\ +(k_{\mathrm{p},j2}+k_{\mathrm{trm},j2})[\mathrm{M}_2] + k_{\mathrm{t},j1}\lambda s_0^1 + k_{\mathrm{t},j2}\lambda s_0^2 \end{array} \right\} \left[\mathrm{SR}_n^j\right] \end{aligned} \tag{B10}$$

Terminated sequences of n units of monomer j

$$\begin{aligned} X_{\mathrm{SP}_n^j} = & \left(k_{\mathrm{trm},j1}[\mathrm{M}_1] + k_{\mathrm{trm},j2}[\mathrm{M}_2] + k_{\mathrm{p},j\left((2-j)\delta_{j,1}+(j-1)\delta_{j,2}\right)}\left[\mathrm{M}_{\left((2-j)\delta_{j,1}+(j-1)\delta_{j,2}\right)}\right]\right)\left[\mathrm{SR}_n^j\right] \\ & + k_{\mathrm{t},j\left((2-j)\delta_{j,1}+(j-1)\delta_{j,2}\right)}\lambda s_0^{\left((2-j)\delta_{j,1}+(j-1)\delta_{j,2}\right)}\left[\mathrm{SR}_n^j\right] \\ & + \left(\tfrac{1}{2}\right)k_{\mathrm{t},jj}\sum_{l=1}^{n-l}\left[\mathrm{SR}_{n-l}^j\right]\left[\mathrm{SR}_l^j\right](1-\delta_{n,1}) \end{aligned} \tag{B11}$$

ath, bth order moment of the sequence of monomer j ending in a capped radical center ($a = 0, 1, 2$)

$$X_{\mu s_a^j} = k_{\mathrm{cap},j}[\mathrm{Te}]\lambda s_a^j - k_{\mathrm{uncap},j}\mu s_a^j \tag{B12}$$

ath, bth order moment of the sequence of monomer j ending in an active radical center ($a = 0, 1, 2$)

$$\begin{aligned} X_{\lambda s_a^j} = & 2fk_{\mathrm{d}}[\mathrm{I}]\left(\frac{[\mathrm{M}_j]}{[\mathrm{M}_1]+[\mathrm{M}_2]}\right) + k_{\mathrm{th}}[\mathrm{M}_j]^3(1+2^a)\delta_{j,1} + k_{\mathrm{p},jj}[\mathrm{M}_j]\sum_{h=0}^{a}\binom{a}{h}\lambda s_{a-h}^j \\ & + \left(k_{\mathrm{p},\left((2-j)\delta_{j,1}+(j-1)\delta_{j,2}\right)j}\lambda s_0^{\left((2-j)\delta_{j,1}+(j-1)\delta_{j,2}\right)} + k_{\mathrm{trm},1j}\lambda s_0^1 + k_{\mathrm{trm},2j}\lambda s_0^2\right)[\mathrm{M}_j] \\ & + k_{\mathrm{uncap},j}\mu s_{a,b}^j + k_{\mathrm{p},j}^{-1}\left\{\left[\mathrm{SR}_1^j\right](1-0^a) - \lambda s_a^j + \sum_{h=0}^{a}\binom{a}{h}(-1)^{a-h}\lambda s_h^j\right\}\delta_{j,2} \\ & - \left\{ \begin{array}{c} (k_{\mathrm{p},j1}+k_{\mathrm{trm},j1})[\mathrm{M}_1] + (k_{\mathrm{p},j2}+k_{\mathrm{trm},j2})[\mathrm{M}_2] \\ +k_{\mathrm{cap},j}[\mathrm{Te}] + k_{\mathrm{t},j1}\lambda s_0^1 + k_{\mathrm{t},j2}\lambda s_0^2 \end{array} \right\}\lambda s_a^j \end{aligned} \tag{B13}$$

ath, bth order moment of the terminated sequence of monomer j

$$\begin{aligned} X_{\varepsilon s_a^j} = & \left(k_{\mathrm{trm},j1}[\mathrm{M}_1] + k_{\mathrm{trm},j2}[\mathrm{M}_2] + k_{\mathrm{p},j\left((2-j)\delta_{j,1}+(j-1)\delta_{j,2}\right)}\left[\mathrm{M}_{\left((2-j)\delta_{j,1}+(j-1)\delta_{j,2}\right)}\right]\right)\lambda s_a^j \\ & + k_{\mathrm{t},j\left((2-j)\delta_{j,1}+(j-1)\delta_{j,2}\right)}\lambda s_0^{\left((2-j)\delta_{j,1}+(j-1)\delta_{j,2}\right)}\lambda s_a^j + \left(\tfrac{1}{2}\right)k_{\mathrm{t},jj}\sum_{h=0}^{a}\binom{a}{h}\lambda s_{a-h}^j\lambda s_h^j \end{aligned} \tag{B14}$$

Appendix C: Kinetic Parameters and Equations for Density and Average Properties

Kinetic constants

$$k_{\mathrm{d}}(\mathrm{min}^{-1}) = 4.92773 \times 10^{15}\cdot\exp\left(-\frac{30000}{1.987\cdot T}\right) \quad [22] \tag{C1}$$

$$f = 0.62 \quad [22] \tag{C2}$$

$$k_{th}(L^2 \cdot mol^{-2} \cdot min^{-1}) = 4.0894965 \times 10^6 \cdot \exp\left(\frac{-13910}{T}\right) \quad [22] \tag{C3}$$

$$k_{p,11}(L \cdot mol^{-1} \cdot min^{-1}) = 2.230379 \times 10^9 \cdot \exp\left(\frac{-7769.17}{1.987 \cdot T}\right) \quad [22] \tag{C4}$$

$$k_{p,22}(L \cdot mol^{-1} \cdot min^{-1}) = 5.9497115 \times 10^{10} \cdot \exp\left(\frac{-13000}{1.987 \cdot T}\right) \quad [22] \tag{C5}$$

$$r_1 = 0.545 \quad [22] \tag{C6}$$

$$r_2 = 0.013 \quad [22] \tag{C7}$$

$$k_{p,12}(L \cdot mol^{-1} \cdot min^{-1}) = \frac{k_{p,11}}{r_1} \tag{C8}$$

$$k_{p,21}(L \cdot mol^{-1} \cdot min^{-1}) = \frac{k_{p,22}}{r_2} \tag{C9}$$

The model takes into account that only macroradicals having two successive AMS (terminal and penultimate) units depropagate.[35] Hence,

$$k_{p,1}^{-1} = 0 \tag{C10}$$

$$k_{p,2}^{-1}(L \cdot mol^{-1} \cdot min^{-1}) = \frac{k_{p,22}}{\exp\left(\frac{29100 - 104 \cdot T}{8.314 \cdot T}\right)} \quad [20] \tag{C11}$$

Besides, the concentration of macroradicals ending in an AMS unit has to be affected by the probability that these macroradicals have an AMS–AMS end sequence in the depropagation rate expression. This probability can be calculated as follows:

$$p_{22} = \frac{\lambda s_0^2 - [SR_1^2]}{\lambda_{0,0}^2} \tag{C12}$$

The remaining kinetic constants are:

$$k_{trm,11}(L \cdot mol^{-1} \cdot min^{-1}) = k_{p,11} \cdot 0.97021918 \cdot \exp\left(\frac{-2820}{T}\right) \quad [22] \tag{C13}$$

$$k_{trm,22}(L \cdot mol^{-1} \cdot min^{-1}) = k_{p,22} \cdot 1.17697688 \times 10^{-4} \quad [22] \tag{C14}$$

$$k_{trm,12}(L \cdot mol^{-1} \cdot min^{-1}) = k_{p,12} \cdot \frac{k_{trm,22}}{k_{p,22}} \quad [22] \tag{C15}$$

$$k_{trm,21}(L \cdot mol^{-1} \cdot min^{-1}) = k_{p,21} \cdot \frac{k_{trm,11}}{k_{p,11}} \quad [22] \tag{C16}$$

$$k_{cap,1}(L \cdot mol^{-1} min^{-1}) = k_{cap,2} = 5.07045126 \times 10^{11} \cdot \exp\left(\frac{-3722}{1.987 \cdot T}\right) \quad [22] \tag{C17}$$

$$k_{uncap,1}(L \cdot mol^{-1} \cdot min^{-1}) = k_{uncap,2} = 2.124504 \times 10^{15} \cdot \exp\left(-\frac{29683}{1.987 \cdot T}\right) \quad [22] \tag{C18}$$

$$k_{t,11}(L \cdot mol^{-1} \cdot min^{-1}) = 5.6903x10^{-8} \cdot (k_{p,11})^2 \cdot \exp\left(\frac{12452.2}{1.987 \cdot T}\right) \cdot (f_{gel})^2 \quad [22] \tag{C19}$$

$$k_{t,22}(L \cdot mol^{-1} \cdot min^{-1}) = 3.7263175 \times 10^{11} \cdot \exp\left(-\frac{2000}{1.987 \cdot T}\right) \cdot (f_{gel})^2 \quad [22] \tag{C20}$$

$$k_{t,12}(L \cdot mol^{-1} \cdot min^{-1}) = k_{t,21} = 1.61582\sqrt{k_{t,11} \cdot k_{t,22}} \quad [22] \tag{C21}$$

The gel effect factor was calculated as follows:[24]

$$f_{\text{gel}} = \begin{cases} 1 & 0 \le C < 0.3 \\ 0.5093 + 2.4645 \cdot C - 3.7473 \cdot C^2 & C \le 0.3 \end{cases} \tag{C22}$$

In order to avoid numerical issues resulting from the discontinuous nature of the gel effect expression, a smoothing was applied:

$$f_{\text{gel}} = 0.5 \cdot \left(0.5093 + 2.4645 \cdot C - 3.7473 \cdot C^2\right) \cdot \{\tanh[3 \cdot (C - 0.3)] + 1\} + 0.5 \cdot \{\tanh[3 \cdot (-C + 0.3)] + 1\} \tag{C23}$$

Densities

$$\rho_{\text{mix}} = \left(\frac{x_{\text{St}}}{\rho_{\text{St}}} + \frac{x_{\text{AMS}}}{\rho_{\text{AMS}}} + \frac{x_{\text{I}}}{\rho_{\text{I}}} + \frac{x_{\text{Te}}}{\rho_{\text{Te}}} + \frac{x_{\text{homoPS}}}{\rho_{\text{homoPS}}} + \frac{x_{\text{homoPAMS}}}{\rho_{\text{homoPAMS}}}\right)^{-1} \tag{C24}$$

$$\rho_{\text{St}} = 919.3 - 0.665 \cdot T(^\circ\text{C}) = \rho_{\text{I}} = \rho_{\text{Te}}; \quad \rho_{\text{AMS}} = 909.0 - 0.265 \cdot T(^\circ\text{C}) \tag{C25}$$

$$\rho_{\text{homoPS}} = 992.6 - 0.265 \cdot T(^\circ\text{C}); \; \rho_{\text{homoPAMS}} = 990.0 - 0.265 \cdot T(^\circ\text{C}) \tag{C26}$$

Average molecular weights

Global number-average molecular weight

$$\overline{M}_{\text{nT}} = \frac{(\mu^1_{1,0} + \mu^2_{1,0} + \lambda^1_{1,0} + \lambda^2_{1,0} + \varepsilon_{1,0})\text{MW}_1 + (\mu^1_{0,1} + \mu^2_{0,1} + \lambda^1_{0,1} + \lambda^2_{0,1} + \varepsilon_{0,1})\text{MW}_2}{\mu^1_{0,0} + \mu^2_{0,0} + \lambda^1_{0,0} + \lambda^2_{0,0} + \varepsilon_{0,0}} \tag{C27}$$

Global weight-average molecular weight

$$\overline{M}_{\text{wT}} = \frac{\left\{\begin{array}{c} (\text{MW}_1)^2\left(\mu^1_{2,0} + \mu^2_{2,0} + \lambda^1_{2,0} + \lambda^2_{2,0} + \varepsilon_{2,0}\right) \\ +2 \cdot \text{MW}_1 \cdot \text{MW}_2\left(\mu^1_{1,1} + \mu^2_{1,1} + \lambda^1_{1,1} + \lambda^2_{1,1} + \varepsilon_{1,1}\right) \\ +(\text{MW}_2)^2\left(\mu^1_{0,2} + \mu^2_{0,2} + \lambda^1_{0,2} + \lambda^2_{0,2} + \varepsilon_{0,2}\right) \end{array}\right\}}{\left\{\begin{array}{c} \text{MW}_1\left(\mu^1_{1,0} + \mu^2_{1,0} + \lambda^1_{1,0} + \lambda^2_{1,0} + \varepsilon_{1,0}\right) \\ +\text{MW}_2\left(\mu^1_{0,1} + \mu^2_{0,1} + \lambda^1_{0,1} + \lambda^2_{0,1} + \varepsilon_{0,1}\right) \end{array}\right\}} \tag{C28}$$

Number average-molecular weight of the dormant chains

$$\overline{M}_{\text{nD}} = \frac{\left(\mu^1_{1,0} + \mu^2_{1,0}\right)\text{MW}_1 + \left(\mu^1_{0,1} + \mu^2_{0,1}\right)\text{MW}_2}{\mu^1_{0,0} + \mu^2_{0,0}} \tag{C29}$$

Weight-average molecular weight of the dormant chains

$$\overline{M}_{\text{wD}} = \frac{(\text{MW}_1)^2\left(\mu^1_{2,0} + \mu^2_{2,0}\right) + 2 \cdot \text{MW}_1 \cdot \text{MW}_2\left(\mu^1_{1,1} + \mu^2_{1,1}\right) + (\text{MW}_2)^2\left(\mu^1_{0,2} + \mu^2_{0,2}\right)}{\left(\mu^1_{1,0} + \mu^2_{1,0}\right)\text{MW}_1 + \left(\mu^1_{0,1} + \mu^2_{0,1}\right)\text{MW}_2} \tag{C30}$$

Number-average molecular weight of the dead chains

$$\overline{M}_{\text{nP}} = \frac{\varepsilon_{1,0} \cdot \text{MW}_1 + \varepsilon_{0,1} \cdot \text{MW}_2}{\varepsilon_{0,0}} \tag{C31}$$

Weight-average molecular weight of the dead chains

$$\overline{M}_{\mathrm{wP}} = \frac{(\mathrm{MW}_1)^2\varepsilon_{2,0} + 2\cdot\mathrm{MW}_1\cdot\mathrm{MW}_2\cdot\varepsilon_{1,1} + (\mathrm{MW}_1)^2\varepsilon_{0,2}}{\varepsilon_{1,0}\mathrm{MW}_1 + \varepsilon_{0,1}\mathrm{MW}_2} \tag{C32}$$

Polydispersity index

$$\mathrm{PDI}_j = \frac{\overline{M}_{\mathrm{w}j}}{\overline{M}_{\mathrm{n}j}} \quad j = T, D, P \tag{C33}$$

Conversion

Global conversion

$$C = \frac{\left\{\begin{array}{c}\mu^1_{1,0} + \mu^2_{1,0} + \lambda^1_{1,0} + \lambda^2_{1,0} + \varepsilon_{1,0} \\ +\mu^1_{0,1} + \mu^2_{0,1} + \lambda^1_{0,1} + \lambda^2_{0,1} + \varepsilon_{0,1}\end{array}\right\}}{\left\{\begin{array}{c}\mu^1_{1,0} + \mu^2_{1,0} + \lambda^1_{1,0} + \lambda^2_{1,0} + \varepsilon_{1,0} + \mu^1_{0,1} \\ +\mu^2_{0,1} + \lambda^1_{0,1} + \lambda^2_{0,1} + \varepsilon_{0,1} + [\mathrm{M}_1] + [\mathrm{M}_2]\end{array}\right\}} \times 100 \tag{C34}$$

Conversion of monomer j

$$C_j = \frac{\mu^1_{1,0} + \mu^2_{1,0} + \lambda^1_{1,0} + \lambda^2_{1,0} + \varepsilon_{1,0}}{\mu^1_{1,0} + \mu^2_{1,0} + \lambda^1_{1,0} + \lambda^2_{1,0} + \varepsilon_{1,0} + [\mathrm{M}_j]} \times 100 \tag{C35}$$

Composition (Styrene)

Instantaneous composition

$$\mathrm{Inst\_Comp} = \frac{k_{\mathrm{p},11}[\mathrm{M}_1]\lambda^1_{0,0} + k_{\mathrm{p},21}[\mathrm{M}_1]\lambda^2_{0,0}}{\left\{\begin{array}{c}k_{\mathrm{p},11}[\mathrm{M}_1]\lambda^1_{0,0} + k_{\mathrm{p},21}[\mathrm{M}_1]\lambda^1_{0,0} + k_{\mathrm{p},12}[\mathrm{M}_2]\lambda^1_{0,0} \\ +k_{\mathrm{p},22}[\mathrm{M}_2]\lambda^2_{0,0} - k^{-1}_{\mathrm{p},2}p_{22}\lambda^2_{0,0}\end{array}\right\}} \tag{C36}$$

Number average global composition

$$\mathrm{Comp\_n} = \frac{\mu^1_{1,0} + \mu^2_{1,0} + \lambda^1_{1,0} + \lambda^2_{1,0} + \varepsilon_{1,0}}{\mu^1_{1,0} + \mu^2_{1,0} + \lambda^1_{1,0} + \lambda^2_{1,0} + \varepsilon_{1,0} + \mu^1_{0,1} + \mu^2_{0,1} + \lambda^1_{0,1} + \lambda^2_{0,1} + \varepsilon_{0,1}} \tag{C37}$$

Appendix D: 2D pgf Modeling Method for Predicting the Bivariate MWD

Population balance equations describe polymer species by a set of distributed molecular properties. When solving these balances, molecular property distributions are obtained. We are interested in obtaining the concentration of polymeric species for given ranges of two variables: n_1 which is the number of monomer 1 units in the copolymer, and n_2 which is the number of monomer 2 units in the copolymer. Hence, we wish to acquire a 2D distribution.

Usually, direct solution of the mass balances is not feasible because the balances commonly form a coupled system of equations in which n_1 and n_2 have to be parameterized for all their possible values, which in theory range from one to infinity. Even though finite upper bounds for n_1 and n_2 may be set according to particular criteria, the system of equations is

usually too large to be tractable. Thus, we employed a method based on the transformation of the infinite population balances governing the polymerization process into the pgf domain, obtaining a system of equations in which the dependent variable is the pgf transform of the distribution. Pgf values are obtained by solving this system, and they are input to an inversion formula in order to recover the desired distribution. In this way, only pgf evaluations at a relatively coarse grid of their dummy variables z_1 and z_2 are required for recovering the distribution for a set of arbitrary values of its independent variables n_1 and n_2. Hence, a finite and reasonably sized system of equations needs to be solved. The pgf equations for any (n_1,n_2) point of the MWD grid are independent of the ones for any other point, which means that the grid of the MWD can be made as sparse as desired, and that this grid can be divided into separate subsections for calculating the complete MWD. This allows adjusting the size of the mathematical model. In the simulations presented in this work, around 12 subsections of approximately 10 by 10 points were employed to reconstruct the MWDs.

The bivariate pgf of order a,b ($\Omega_{a,b}$) of species Y with n_1 units of monomer 1 and n_2 units of monomer 2 is defined as follows:

$$\Omega_{a,b}(z_1,\ z_2) = \sum_{n_1=0}^{\infty} {z_1}^{n_1} {n_1}^{a} \sum_{n_2=0}^{\infty} {z_2}^{n_2} {n_2}^{b} \frac{\left[\mathrm{Y}_{n_1,n_2}\right]}{\kappa_{a,b}} \tag{D1}$$

where $\kappa_{a,b}$ is the double index moment of order a,b of species $Y_{n1,n2}$ while z_1 and z_2 are the dummy variables of the pgf.

Following the procedure outlined in Asteasuain and Brandolin,[34] the mass balances of the polymer species are transformed into the 2D pgf domain obtaining the corresponding pgf balances. These balances have the general structure shown in Equation (A3) and (A7), while the corresponding reaction rates for the 0,0 pgfs are:
for the dormant copolymer with a monomer j final unit

$$X_{\mu^j_{0,0}\varphi^j_{0,0}}(z_1,z_2) = k_{\mathrm{cap},j}[\mathrm{Te}][\lambda^j_{0,0}\sigma^j_{0,0}(z_1,z_2)] - k_{\mathrm{uncap,j}}[\mu^j_{0,0}\varphi^j_{0,0}(z_1,z_2)] \tag{D2}$$

for the macroradical with a monomer j final unit

$$\begin{aligned} X\lambda^j_{0,0}\sigma^j_{0,0}(z_1,z_2) = {} & \left\{ \begin{array}{l} 2fk_d[I]\left(\frac{[\mathrm{M}_j]}{[\mathrm{M}_1]+[\mathrm{M}_2]}\right) \\ +(k_{\mathrm{trm},1j}\lambda^1_{0,0} + k_{\mathrm{trm},2j}\lambda^2_{0,0})[\mathrm{M}_j] \end{array} \right\}(z_1\delta_{j,1} + z_2\delta_{j,2}) \\ & +k_{\mathrm{th}}[\mathrm{M}_j]^3(z_1 + 2z_1^2)\delta_{j,1} + k_{\mathrm{uncap,j}}[\mu^j_{0,0}\varphi^j_{0,0}(z_1,z_2)] + \\ & \quad \frac{k^{-1}_{\mathrm{p,j}}p_{22}}{z_2}[\lambda^j_{0,0}\sigma^j_{0,0}(z_1,z_2)]\delta_{j,2} \\ & +k_{\mathrm{p,1j}}[\mathrm{M}_j]\{z_1[\lambda^1_{0,0}\sigma^1_{0,0}(z_1,z_2)]\delta_{j,1} + z_2[\lambda^1_{0,0}\sigma^1_{0,0}(z_1,z_2)]\delta_{j,2}\} \\ & +k_{\mathrm{p,2j}}[\mathrm{M}_j]\{z_1[\lambda^2_{0,0}\sigma^2_{0,0}(z_1,z_2)]\delta_{j,1} + z_2[\lambda^2_{0,0}\sigma^2_{0,0}(z_1,z_2)]\delta_{j,2}\} \end{aligned} \tag{D3}$$

for the dead copolymer

$$\begin{aligned} X_{\varepsilon_{0,0}\vartheta_{0,0}(z_1,z_2)} = {} & \left(k_{\mathrm{trm},11}[\mathrm{M}_1] + k_{\mathrm{trm},12}[\mathrm{M}_2]\right)\left[\lambda^1_{0,0}\sigma^1_{0,0}(z_1,z_2)\right] \\ & +\left(k_{\mathrm{trm},21}[\mathrm{M}_1] + k_{\mathrm{trm},22}[\mathrm{M}_2]\right)\left[\lambda^2_{0,0}\sigma^2_{0,0}(z_1,z_2)\right] \\ & +k_{\mathrm{t},12}\left[\lambda^1_{0,0}\sigma^1_{0,0}(z_1,z_2)\right]\left[\lambda^2_{0,0}\sigma^2_{0,0}(z_1,z_2)\right] \\ & +\left(\tfrac{1}{2}\right)k_{\mathrm{t},11}\left[\lambda^1_{0,0}\sigma^1_{0,0}(z_1,z_2)\right]^2 + \left(\tfrac{1}{2}\right)k_{\mathrm{t},22}\left[\lambda^2_{0,0}\sigma^2_{0,0}(z_1,z_2)\right]^2 \end{aligned} \tag{D4}$$

After solving the pgf balances, it is possible to calculate the pgf for the overall copolymer as:

$$\tau_{0,0}(z_1,z_2) = \frac{\left\{ \begin{array}{c} \left[\lambda^1_{0,0}\sigma^1_{0,0}(z_1,z_2)\right] + \left[\lambda^2_{0,0}\sigma^2_{0,0}(z_1,z_2)\right] \\ +\left[\mu^1_{0,0}\varphi^1_{0,0}(z_1,z_2)\right] + \left[\mu^2_{0,0}\varphi^2_{0,0}(z_1,z_2)\right] + \left[\varepsilon_{0,0}\vartheta_{0,0}(z_1,z_2)\right] \end{array} \right\}}{\lambda^1_{0,0} + \lambda^2_{0,0} + \mu^1_{0,0} + \mu^2_{0,0} + \varepsilon_{0,0}} \tag{D5}$$

Any bivariate MWD (of the overall copolymer, dormant chains, dead chains, or macroradicals) can be recovered by numerical inversion of its pgf transform. The inversion method used here is described in Asteasuain and Brandolin.[34] The inversion formula is:

$$\mathrm{MWD}_{\mathrm{number}}(n_1, n_2) = \frac{(\ln(2))^2}{n_1 \cdot n_2} \mathbf{v}_1^{\mathrm{T}} \cdot \mathbf{PGF}(\mathbf{z}_1, \mathbf{z}_2) . \mathbf{v}_2^{\mathrm{T}} \tag{D6}$$

where $\mathrm{MWD}_{\mathrm{number}}(n_1,n_2)$ is the bivariate MWD expressed in number fraction of any of the polymer species, and $\mathbf{PGF(z_1,z_2)}$ is a matrix of the corresponding 2D pgf defined as:

$$\mathbf{PGF}(\mathbf{z}_1, \mathbf{z}_2) = \begin{bmatrix} \mathrm{pgf}(z_{1,0}, z_{2,0}) & \mathrm{pgf}(z_{1,0}, z_{2,1}) & \cdots & \mathrm{pgf}(z_{1,0}, z_{2,N2}) \\ \mathrm{pgf}(z_{1,1}, z_{2,0}) & & & \mathrm{pgf}(z_{1,1}, z_{2,N2}) \\ \vdots & & & \vdots \\ \mathrm{pgf}(z_{1,N1}, z_{2,0}) & \mathrm{pgf}(z_{1,N1}, z_{2,1}) & \cdots & \mathrm{pgf}(z_{1,N1}, z_{2,N2}) \end{bmatrix} \tag{D7}$$

$$z_{i,j} = \exp\left(-(2j+1)\frac{\ln(2)}{n_i}\right) \tag{D8}$$

In this expression, N_1 and N_2 are parameters of the method. Besides, $\mathbf{v_1}$ and $\mathbf{v_2}$ are vectors that can be obtained by solving the system of linear equations

$$\mathbf{A}_i \mathbf{v}_i = \mathbf{L}_{2Ni}(1/2) \tag{D9}$$

In this equation, $\mathbf{A}_i$ is a lower triangular matrix of dimensions $(N_i + 1 \times N_i + 1)$ whose elements are defined as:

$$A_{i,k,f} = \sum_{l=0}^{k} \frac{(k-f+1)_f}{2(k+1/2)_{f+1}} \quad f = 0, \ldots, k \text{ and } k = 0, \ldots, Ni \tag{D10}$$

where

$$(j)_h = \begin{cases} 1 & h = 0 \\ j(j+1)\ldots(j+h+1) & h > 0 \end{cases} \tag{D11}$$

$\mathbf{L}_{2Ni}$ is a vector whose elements $L_{2Ni,j}$, $j = 0,\ldots,Ni$ are Legendre polynomials of order $2j$ evaluated at $x = 1/2$. Legendre polynomials are calculated as follows:

$$\begin{aligned} L_0(x) &= 1 \\ L_1(x) &= x \\ &\vdots \\ (l+1)L_{l+1}(x) &= (2l+1)xL_l(x) - lL_{l-1}(x) \end{aligned} \tag{D12}$$

Finally, the $\mathrm{MWD}_{\mathrm{weight}}$ can be obtained from the number fraction distribution according to:

$$\mathrm{MWD}_{\mathrm{weight}}(n_1, n_2) = \left[\frac{(n_1 \mathrm{MW}_1 + n_2 \mathrm{MW}_2) \cdot \begin{pmatrix} \lambda_{0,0}^1 + \lambda_{0,0}^2 + \mu_{0,0}^1 \\ + \mu_{0,0}^2 + \varepsilon_{0,0} \end{pmatrix}}{\begin{pmatrix} \mu_{1,0}^1 + \mu_{1,0}^2 + \lambda_{1,0}^1 + \lambda_{1,0}^1 + \varepsilon_{1,0} \end{pmatrix} \mathrm{MW}_1 + \begin{pmatrix} \mu_{0,1}^1 + \mu_{0,1}^2 + \lambda_{0,1}^1 + \lambda_{0,1}^2 + \varepsilon_{0,1} \end{pmatrix} \mathrm{MW}_2} \right] \cdot \mathrm{MWD}_{\mathrm{number}}(n_1, n_2) \tag{D13}$$

5. Nomenclature

C	global conversion
C_j	conversion of monomer j
Comp_n	number average fraction of monomer 1 (Styrene) in the overall copolymer
$\left[D^j_{n_1,n_2}\right]$	concentration of dormant copolymer with n_1 units of St (1) and n_2 units of AMS (2) ended in monomer j
f	initiator efficiency
f_{gel}	gel factor
$F_{\text{sb,lat}}$	continuous feed flow rate for semibatch reactor ($g \cdot min^{-1}$)
$F_{\text{tub,lat}}$	side feed flux per unit length for tubular reactor ($g \cdot L^{-1} \cdot min^{-1}$)
[I]	concentration of initiator
Inst_comp	instantaneous composition, average fraction of monomer 1 (Styrene) in the copolymer being formed.
k_i	kinetic constant of generic reaction i
$[M_j]$	concentration of monomer j ($j=1$: styrene and $j=2$: α-methylstyrene)
$\overline{M}_{\text{ni}}$	number average molecular weight of generic species i
$\text{MWD}_{\text{number}}$	number average molecular weight distribution
$\text{MWD}_{\text{weight}}$	weight average molecular weight distribution
$\overline{M}_{\text{wi}}$	weight average molecular weight of generic species i
MW_i	molecular weight of generic species i
p_{22}	fraction of active radicals ending in an AMS unit that have an AMS-AMS end sequence
PDI_i	polidispersity index of generic species i
$[P_{n_1,n_2}]$	concentration of dead copolymer with n_1 units of St (1) and n_2 units of AMS (2).
r_j	reactivity ratio of component j
$\left[R^j_{n_1,n_2}\right]$	concentration of macroradical chain with n_1 units of St (1) and n_2 units of AMS (2) ended in monomer j
$\left[SD^j_n\right]$	concentration of sequence of dormant copolymer with n units of monomer j
$\left[SP^j_n\right]$	concentration of terminated sequence with n units of monomer j
$\left[SR^j_n\right]$	concentration of sequence of macroradical chain with n units of monomer j
t	residence time
[Te]	concentration of mediator (TEMPO)
v	axial velocity in tubular reactor
V	reaction volume in batch or semibatch reactor
x_i	mass fraction of generic species i
X_i	reaction rate of generic species i
y_i	number fraction of generic species i
$[Y_{n_1,n_2}]$	concentration of a species with n_1 units of St (1) and n_2 units of AMS (2).
z	axial distance in tubular reactor

6. Greek Symbols

$\delta_{n,a}$	Kronecker delta
$\varepsilon_{a,b}$	ath, bth order moment of dead copolymer
εs^j_a	ath order moment of terminated sequence of monomer j
$\vartheta^j_{a,b}(z_1, z_2)$	ath, bth order pgf of dead copolymer
$\lambda^j_{a,b}$	ath, bth order moment of macroradical chain ended in monomer j
λs^j_a	ath order moment of active radical sequence of monomer j
$\mu^j_{a,b}$	ath, bth order moment of dormant copolymer ended in monomer j
μs^j_a	ath order moment of dormant sequence of monomer j
ρ_i	density of generic species i
$\sigma^j_{a,b}(z_1, z_2)$	ath, bth order pgf of macroradical chain ended in monomer j
$\tau_{a,b}(z_1, z_2)$	ath, bth order pgf of the overall copolymer
$\varphi^j_{a,b}(z_1, z_2)$	ath, bth order pgf of dormant copolymer ended in monomer j

Acknowledgements: The authors acknowledge the financial support of CONICET (National Research Council of Argentina), ANPCyT (National Agency for Promotion of Science and Technology of Argentina), and UNS (Universidad Nacional del Sur).

Received: December 7, 2012; Revised: February 26, 2013; Published online: DOI: 10.1002/mren.201200084

Keywords: copolymerization; modeling; molecular weight distribution; nitroxide mediated polymerization; pgf

[1] W. A. Braunecker, K. Matyjaszewski, *Prog. Polym. Sci.* **2007**, *32*, 93.
[2] R. Wang, Y. Luo, B. Li, X. Sun, S. Zhu, *Macromol. Theory Simul.* **2006**, *15*, 356.
[3] R. Wang, Y. Luo, B. G. Li, S. Zhu, *AICHE J.* **2007**, *53*, 174.
[4] J. F. Lutz, T. Pakula, K. Matyjaszewski, *ACS Symp. Ser.* **2003**, *854*, 268.
[5] K. Matyjaszewski, K. A. Davis, "*Statistical, Gradient, Block and Graft Copolymers by Controlled/Living Radical Polymerizations*", Springer-Verlag, Berlin, Germany **2002**.

[6] D. Konkolewicz, M. Siauw, A. Gray-Weale, B. S. Hawkett, S. Perrier, *J. Phys. Chem. B* **2009**, *113*, 7086.
[7] B. K. Denizli, J. F. Lutz, L. Okrasa, T. Pakula, A. Guner, K. Matyjaszewski, *J. Polym. Sci., Part A: Polym. Chem.* **2005**, *43*, 3440.
[8] J. M. G. Cowie, M. D. Fernandez, M. J. Fernandez, I. J. McEwen, *Polymer* **1992**, *33*, 2744.
[9] M. Zhang, W. H. Ray, *J. Appl. Polym. Sci.* **2002**, *86*, 1630.
[10] M. Zhang, W. H. Ray, *J. Appl. Polym. Sci.* **2002**, *86*, 1047.
[11] Y. Ye, F. J. Schork, *Ind. Eng. Chem. Res.* **2009**, *48*, 10827.
[12] Y. Ye, F. J. Schork, *Macromol. React. Eng.* **2010**, *4*, 197.
[13] L. Wang, L. J. Broadbelt, *Macromolecules* **2009**, *42*, 7961.
[14] L. Wang, L. J. Broadbelt, *Macromolecules* **2010**, *43*, 2228.
[15] L. Wang, L. J. Broadbelt, *Macromol. Theory Simul.* **2011**, *20*, 191.
[16] G. Papavasiliou, F. Teymour, *Macromol. Theory Simul.* **2003**, *12*, 543.
[17] A. Krallis, D. Meimaroglou, C. Kiparissides, *Chem. Eng. Sci.* **2008**, *63*, 4342.
[18] J. B. P. Soares, A. E. Hamielec, *Macromol. Theory Simul.* **1997**, *6*, 591.
[19] C. Schütte, M. Wulkow, *Macromol. React. Eng.* **2010**, *4*, 562.
[20] D. Kukulj, T. P. Davis, *Macromolecules* **1998**, *31*, 5668.
[21] D. Kukulj, T. P. Davis, R. G. Gilbert, *Macromolecules* **1998**, *31*, 994.
[22] M. Asteasuain, D. Covan, C. Sarmoria, A. Brandolin, C. Leite de Araujo, J. C. Pinto, in *21st European Symposium on Computer Aided Process Engineering* Vol. 29, Elsevier, 2011.
[23] M. Asteasuain, S. Matheus, M. K. Lenzi, R. A. Hutchinson, M. Cunningham, A. Brandolin, J. C. Pinto, C. Sarmoria, *Macromol. React. Eng.* **2007**, *1*, 622.
[24] A. Faliks, R. A. Yetter, C. A. Floudas, Y. Wei, H. Rabitz, *Polymer* **2001**, *42*, 2061.
[25] J. P. A. Heuts, G. T. Russell, G. B. Smith, A. M. Van Herk, *Macromol. Symp.* **2007**, *248*, 12.
[26] G. B. Smith, G. T. Russell, M. Yin, J. P. A. Heuts, *Eur. Polym. J.* **2005**, *41*, 225.
[27] K. J. Beers, W. H. Ray, *J. Appl. Polym. Sci.* **2001**, *79*, 266.
[28] F. Lopez-Serrano, J. M. Castro, C. W. Macosko, M. Tirrell, *Polymer* **1980**, *21*, 263.
[29] R. Y. Tabash, F. A. Teymour, J. A. Debling, *Macromolecules* **2006**, *39*, 829.
[30] L. Wang, L. J. Broadbelt, *Macromol. Theory Simul.* **2011**, *20*, 54.
[31] D. J. Arriola, *Ph. D. Thesis*, University of Wisconsin-Madison (Madison, Wisconsin, USA), 1989.
[32] A. Zargar, F. J. Schork, *Ind. Eng. Chem. Res.* **2009**, *48*, 4245.
[33] A. Zargar, F. J. Schork, *Macromol. React. Eng.* **2009**, *3*, 118.
[34] M. Asteasuain, A. Brandolin, *Macromol. Theory Simul.* **2010**, *19*, 342.
[35] C. Barner-Kowollik, T. P. Davis, *Macromol. Theory Simul.* **2001**, *10*, 255.